FINAL TECHNICAL REPORT
Award Number: G19AP00021 and G19AP00022

Charleston Area Earthquake Hazards Mapping Project Time History Database, Urban Hazard Maps, and Public Outreach Workshop: Collaborative Research with University of Memphis and the College of Charleston

Chris H. Cramer
CERI, Univ. of Memphis
3890 Central Ave
Memphis, TN 38152-3050
ccramer@memphis.edu

Steven C. Jaumé
Department of Geology and Environmental Geosciences
College of Charleston
66 George Street
Charleston, SC 29424
JaumeC@cofc.edu

Norman S. Levine
Department of Geology and Environmental Geosciences
College of Charleston
66 George Street
Charleston, SC 29424
LevinN@cofc.edu

January 1, 2019 – December 31, 2019

Submitted: March 31, 2020

"Research supported by the U.S. Geological Survey (USGS), Department of Interior, under USGS award numbers G19AP00021 and G19AP00022. The views and conclusions contained in this document are those of the authors and should not be interpreted as necessarily representing the official policies, either expressed or implied, of the U.S. Government."

Abstract

Urban hazard maps have been generated using state-of-the-art approaches, nonlinear site response, and the 2014 USGS NSHMP source and attenuation models. These hazard maps include the impact of the very soft soils (typically NEHRP Site Class D, E and F in the Charleston region) above the stiff Cooper Marl. Of particular concern in the Charleston region is the differentiating the site response of variable thicknesses of artificial fill and tidal marsh deposits that exist along the many waterways in the region, which we have addressed and refined. Both probabilistic and scenario hazard maps have been generated for the nine-quadrangle study area with higher resolution hazard maps being generated for the Charleston quadrangle where data density is higher. Alternative source models exist for the 1886 M7.0 Charleston earthquake (Dura-Gomez and Talwani, 2009; Chapman et al., 2016; Pratt et al., 2014), so we compared M7.0 PGA hazard maps for the alternatives with the MMI X zone of Bollinger (1977). The 1886 MMI's suggest that all three fault alternatives are possible sources, but the west-dipping fault source is less likely than the other two. The engineering and geotechnical user community in the Charleston area requested a Charleston-area-specific time history database containing a suite of time histories on Cooper Marl (Tertiary clay deposit), which we generated using user community input. The Cooper Marl is the near-surface geologic formation that engineered structures are founded on. The Charleston specific time history database will be very useful for design purposes according to the engineering and geotechnical user community and they indicated that there is strong demand for such a database. Final CAEHMP urban hazard maps and products were presented at quarterly user community workshops and all products are available from the Lowcountry Hazards Center using the links provided in the story map at (https://arcg.is/1nPWuy).

Introduction

Statewide seismic hazard maps that include the effect of regional geology have been produced by Silva et al. (2003) for the State of South Carolina, and Chapman and Talwani (2002) for the South Carolina Department of Transportation. These statewide maps model the thickening Atlantic coastal sediments and the general distribution of thinner sediments inland, but do not model the detailed shallow geology needed for urban seismic hazard maps. In recent years, new studies have improved the understanding of both seismic site response (Andrus et al., 2006; Chapman et al., 2006) and liquefaction potential (Hayati and Andrus, 2008; Heidari and Andrus, 2010; Juang and Li, 2007) in the Charleston, SC region. The studies cited above are based mainly upon geotechnical data in the Charleston region. Ground motion records from the Charleston region are still scarce. A small but growing number of records from both local (e.g., Dec. 16, 2008 M = 3.6 Summerville, SC) and regional (e.g., Aug. 23, 2011 M = 5.8 Mineral, VA and March 19, 2014 M = 3.0 Lincolnville, SC) earthquakes have been recorded at the four ANSS strong motion sites in Charleston plus, for the 2014 event, USArray stations in the surrounding region. The strong motion sites have been characterized by both geotechnical and surface seismic means (Jaumé, 2006). New ambient noise ground motion records also exist at ~75 sites in Charleston, most close to locations of pre-existing geotechnical boreholes (Miner and Jaumé, 2011). Horizontal to vertical spectral ratio (HVSR) estimates of resonance frequencies from ambient seismic noise match estimates derived from geotechnical data at frequencies < 2 Hz but

disagree at higher frequencies (Jaumé and Miner, 2011). Work still needs to be done to bring the geotechnical and seismic estimates of site response into agreement, which has been done successfully in other areas (e.g., Motazedian et al, 2011). The USGS has also funded continuing 1886 seismic source studies both internally (Tom Pratt) and externally (Lee Liberty) to identify the probable location of the fault ruptures in the 1886 M7.0 Charleston, SC earthquake, which are continuing.

Toward this end, the Charleston Area Earthquake Hazards Mapping Project (CAEHMP) Community Velocity Model development (grant G16AP00025) and Liquefaction Probability analysis (grant G16AP00118) have improved the ability to generate urban seismic hazard maps for the nine-quadrangle study area covering the densest population of the three county Charleston area (Figure 1). Figure 2 presents new depth to seismic basement and top of the Cooper Marl maps developed for the CAEHMP Community Velocity Model, together with the geophysical, geotechnical, and geological boring coverage used in their development (Jaumé et al., 2015, 2016; Jaumé and Levine, 2018).

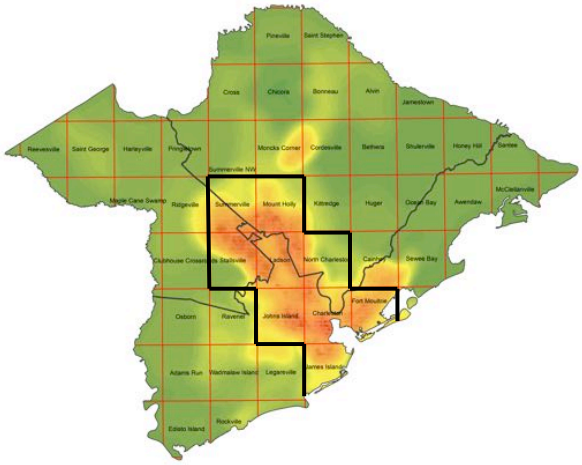

Figure 1: Urban hazard mapping area for CAEHMP based on recent population growth. Areas of red have the highest population growth in the last decade.

In addition to new maps of major geological boundaries that control site response, the CAEHMP Community Velocity Model also makes use of V_S measurements from 3 deep (≥ 500 feet) geotechnical boreholes in the Atlantic coastal plain sponsored by the South Carolina Department of Transportation. All of these boreholes (Figure 3) show an increase in shear wave velocity to ~900 m/sec in the Santee Limestone/Chicora Member (Williamsburg Fm.), followed by a sharp decrease to ~450 m/sec in the underlying Lower Bridge Member (Williamsburg Fm.) for the 2 boreholes that penetrate through this layer. The upper part of the CAEHMP Community Velocity Model is therefore significantly different both from those used in earlier state-wide studies (Chapman and Talwani, 2002; Silva et al., 2003) and in the CAEHMP pilot study (Cramer et al., 2015).

The CAEHMP Community Velocity Model has also updated V_S profiles for surficial geologic units. A greater variety of surficial units exist in the 9 CAEHMP study region than were used in the initial pilot study that only covered the Charleston quadrangle. An important result of the CAEHMP pilot study (Cramer et al., 2015) was that different surficial geologic units have very

similar site response and can usefully be grouped together. Geotechnical data gathered for the CAEHMP Community Velocity Model (Jaumé et al., 2016) has also confirmed prior suspicions that the "artificial fill" site category will need to be split into at least 2 subcategories to account for differences in sub-fill materials (e.g., tidal marsh vs Quaternary sand deposits). This will be potentially important in the Charleston and North Charleston quadrangles, which are underlain by a paleo-drainage of the Cooper River and host numerous port, industrial and military facilities, as well as historic downtown Charleston.

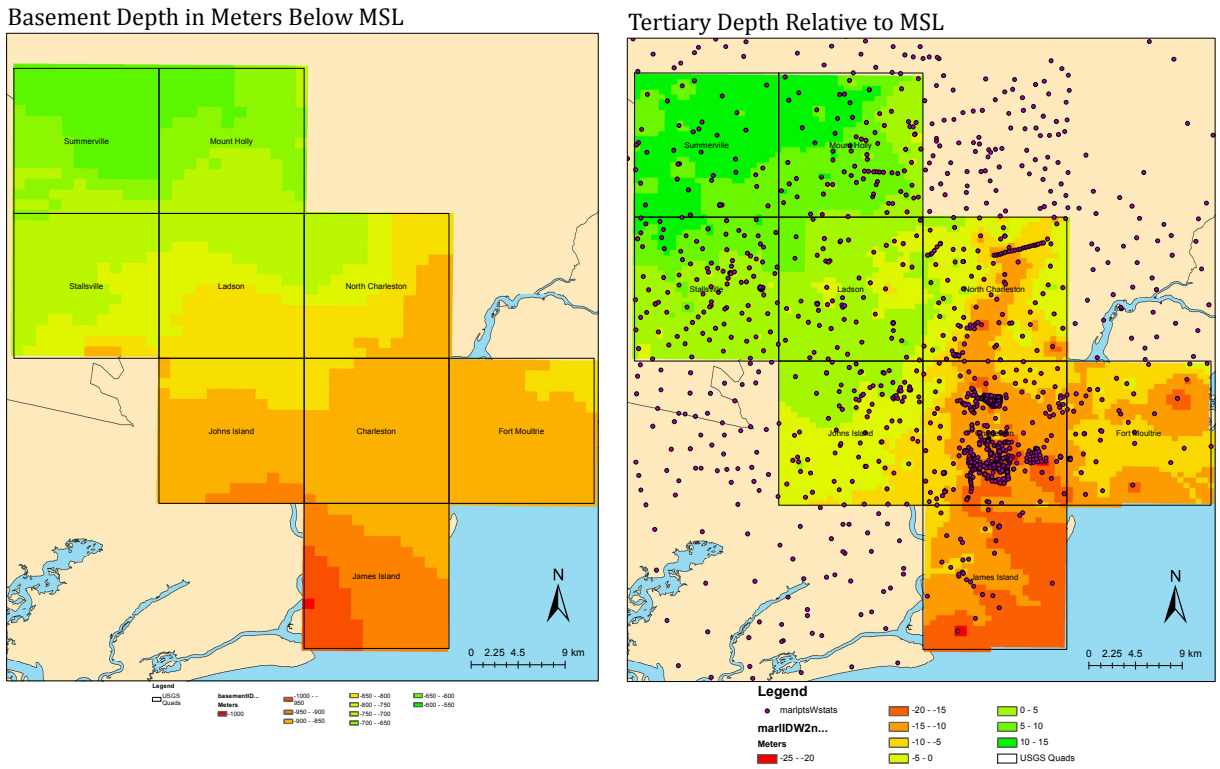

Figure 2: Left: Depth to Paleozoic bedrock (basalt and sedimentary rocks) derived from water well and seismic refraction/reflection data. Right: Elevation to the top of the Tertiary Cooper Marl (dense clay) in the CAEHMP study area with location of geological and geotechnical borings.

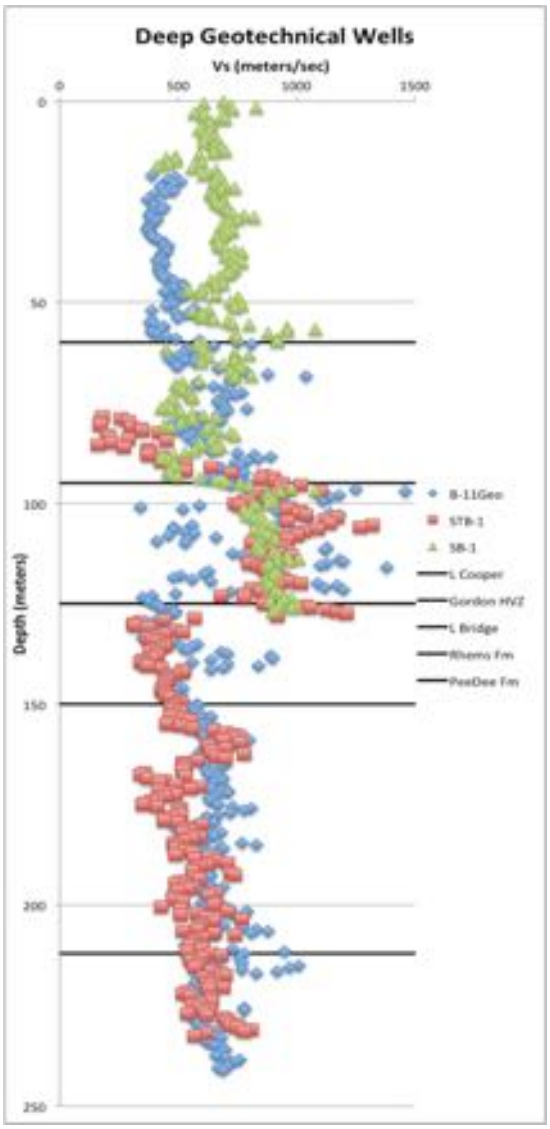

Figure 3: Shear wave velocity with depth in 3 geotechnical boreholes in the Atlantic Coastal Plain in South Carolina (Depths in STB-1 & SB-1 have been shifted to match B-11Geo). A 25-35 meter thick ~900 m/sec layer is encountered is all boreholes, followed by a drop to ~450 m/sec in the 2 boreholes that penetrate beneath this layer.

The initial pilot project (Cramer et al., 2015) laid out an overall project master plan involving seven major tasks: (1) community velocity model development, (2) liquefaction probability analysis, (3) a Charleston specific time history database, (4) urban hazard maps, (5) HAZUS analysis, (6) outreach, and (7) project administration and data management. The first two tasks were completed by the end of 2017 for the community velocity model (grant G16AP00025) and by early 2018 for the liquefaction probability analysis (grant G16AP00118). This study focuses on the development of a Charleston specific time history database requested by the user community at the initial workshop (major task 3), on generating seismic and liquefaction hazard maps for an initial set of nine quadrangles and comparing them to the 1886 earthquake intensity maps (major task 4), and on holding a community outreach workshop (major task 6) plus project administration (major task 7).

Methodologies

Earthquake ground motions at any location (CAEHMP major tasks 3 and 4) basically depend on the size of the earthquake (magnitude), how ground motions decay with distance from the earthquake faulting (attenuation with distance), and how soils beneath a site increase or decrease certain frequencies in the ground motion (site amplification based on local geology). Earthquake hazard estimates (CAEHMP major task 4) basically depend on the rate at which earthquakes occur in the region surrounding a site (recurrence) and the magnitudes of those earthquakes. Larger earthquakes have bigger associated ground motions over a wider area and hence can cause more damage and pose a greater hazard than smaller earthquakes. Thus, earthquake hazard estimates are dominated by the rate of large earthquakes (magnitude 7's in the central and eastern U.S). For the Charleston seismic zone, dated paleoliquefaction features indicate that M7 earthquakes occur on average every 550 years (Talwani and Schaeffer, 2001), which poses a significant hazard in the eastern U.S.

Probabilistic seismic hazard estimates answer the question "What is the likelihood of a given level of ground shaking being exceeded at a site?" This involves knowing where the earthquakes occur in the region (the distance to each earthquake source from the site) especially the source of the 1886 Charleston SC earthquake, their distribution of magnitudes and how often they occur for each earthquake source (magnitude-frequency distribution), and how big the ground motion is for every earthquake's magnitude and distance from the site (ground motion attenuation relation). The national seismic hazard maps combine the probabilities from these distributions for each earthquake source in the region, but do so for a uniform soil condition (amplification). That is, the national maps do not take into account the effects of local geology on earthquake ground motions, but only consider one site condition that is rare in the CEUS (unlikely to be pertinent).

Urban seismic hazard maps (CAEHMP major task 4) do add in the effect of local geology on the amplification of earthquake ground motions in order to have more realistic ground motions for earthquake hazard analysis within the study area. To do this, information is needed about the local distribution and thicknesses of soil in the urban area, which is provided as part of the Community Velocity Model (CAEHMP major task 1). Basically, two pieces of information are needed: what are the thicknesses at a site of each soil type (lithology) and what are each soil type's physical (geotechnical) properties that affect ground motion amplification. Site amplification at a site is determined by taking a soil profile (soil type, thicknesses and physical properties) and subjecting that soil profile to earthquake shaking (time history) in the solid rock at the bottom of the soil profile to calculate the expected shaking at the surface of the ground. The change in amplitude of the shaking from the bottom to the top of the soil profile is site amplification.

Figure 4 provides a generalized picture of how all the earth science and geological/geotechnical information comes together to generate urban seismic ground motion hazard maps. A lot of information needs to be developed and brought together from a variety of disciplines and sources. Validation and quality control of the information must occur for the urban hazard maps to be realistic and beneficial. The information and procedures must reflect our current

understanding and best available science to be credible so the products can be used with confidence.

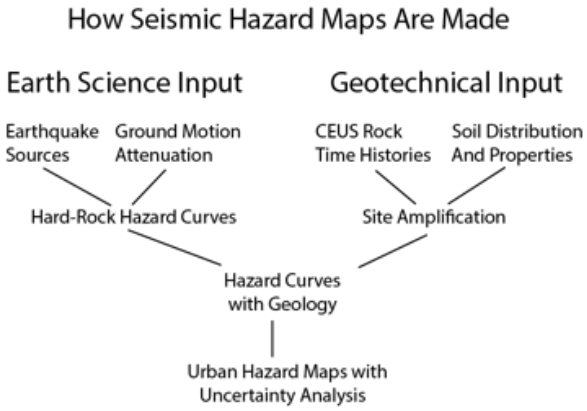

Figure 4: How seismic hazard maps are made.

Modifying hard rock time histories for local site conditions involves the geotechnical input portion of Figure 4. Rock time histories are modified by the local soil distribution and properties using a soil response program. The near-surface soil properties in the Charleston area are saturated, soft soils (Vs < 360 m/s) and Charleston is located close (< 30 km) to a major earthquake source that generated a M7 earthquake in 1886. Thus, the soil response program used to modify time histories, both for a local time history database (CAEHMP major task 3) and for site amplification distributions used in urban hazard map generation (CAEHMP major task 4), needs to be a state-of-the-art nonlinear response programs (Dhar, 2017) like NOAH-IWAN and SeismoSoil, and possibly including the effects of dynamic pore pressure changes like NOAH (Bonilla, 2000; Bonilla et al., 2005). NOAH is a one-dimensional, finite difference code that incorporates pore-pressure generation using stress-strain constitutive models with a general hysteresis formulation (Bonilla et al., 2005). That the inclusion of dynamic pore pressure effects is important is shown (Figure 5) in the comparison of soil response spectra from NOAH-IWAN, a drained nonlinear (no pore pressure effects) program, SeismoSoil, and an equivalent linear program (SHAKE91). We do not see much difference among response spectra for modest input ground motion, but for very strong input ground motion, there are important differences (Figure 5). Equivalent linear programs (SHAKE), although much more computationally efficient than nonlinear programs, do not perform as well at strong ground motion levels (Hartzell et al., 2004). Nonlinear simulation programs have been shown to more reliably predict the soil response, but at a greater computational cost. Nonetheless, in Figure 5 for the Mississippi embayment, nonlinear and equivalent linear soil responses programs using modulus and damping curves show similar site amplifications as a function of period. Dynamic pore pressure effects in a nonlinear approach show higher ground motions then from a drained nonlinear approach for saturated, soft soils due to "strain hardening" effects. However, the Cooper Marl is a stiff clay and does not liquefy. Hence a nonlinear algorithm without pore pressure effects is sufficient for generating the time history database of task 3.

The usefulness of urban seismic hazard maps is also highly dependent on how well the V_S models capture the important details of the near surface soil column. Experience from the CAEHMP pilot study (Figure 6) shows that there can be varying response with increasing soil

thickness for different soil units at different frequencies, as well as potential discontinuities in behavior as a critical soil thickness is reached. In addition, new geotechnical results acquired as part of the CAEHMP Community Velocity Model show that the nature of the material underlying artificial fill can be variable and this will impact the site response at these locations (Jaumé et al., 2016). R. Andrus (pers. comm.) has found that shallow V_S on artificial fill at the former Charleston Naval Base can vary over very short distances. In that case PI Jaumé was able to determine that one V_S profile was underlain by a filled in tidal channel while the other was on Quaternary sand deposits by interrogating historic USGS topographic maps. As a result, the CAEHMP Community Velocity Model team collected historic topographic (and other) maps to aid in this interpretation (see Updated Charleston Quadrangle Surface Geology section).

Additionally, nonlinear (and equivalent linear) soil response results are sensitive to damping at high strains (1% and greater), which has larger uncertainties (Dhar, 2017). Near (less than 30 km) fault sources in the Mississippi embayment, Dhar (2017) and Dhar and Cramer (2017) found that seismic hazard appears high using conventional modulus and damping curves (such as EPRI, 1993). Shi and Asimaki (2017) recently showed that damping at high strains, normally expected to be increasing, can actually plateau or decrease dramatically starting near 0.1% strain. The effect on seismic hazard estimates of inaccuracies in damping at high strains for standard modulus and damping models needs to be investigated for the Charleston area using alternative damping models and actual high strain observations. Observations at high strains for thick soft-soil sites are available to constrain hazard-mapping results from the 2010-2011 Christchurch, NZ earthquake sequence and from earthquakes in Japan for M6-7 earthquakes, which are the magnitudes expected from the Charleston seismic zone ~30 km from downtown Charleston.

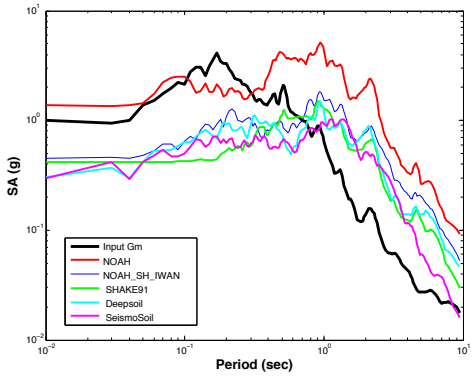

Figure 5: Response spectral ratios for 5% damped condition using different site response programs. Black response spectrum is for the input ground motion (1g) at the bedrock-soil interface.

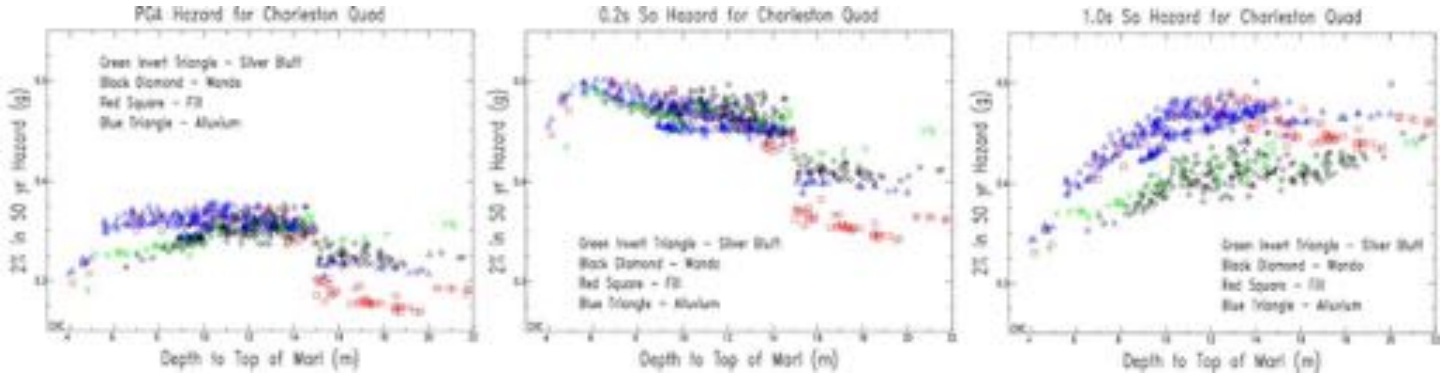

Figure 6: Hazard responses of four Quaternary soil-type columns as a function of thickness (depth to Tertiary dense clay marl) at three periods: PGA (left), 0.2 s (middle), and 1.0 s (right).

The efficiency of the hazard calculations is important because of the large number of grid points at which the calculations are made using a ~500 m grid spacing for the full 9 quadrangle study region and ~100 m grid spacing in the Charleston quadrangle. Efficiencies developed by the Memphis and St. Louis urban hazard mapping will be used in the Charleston project. Similar to the Charleston project with 9 initial hazard maps, the Memphis and St. Louis urban hazard mapping projects provided urban seismic hazard maps for 12+ and 29 quadrangles, respectively. For a given site, the probability, P(A > Ao), of exceeding a specific ground motion Ao (Reiter, 1990, equation 10.2) is given by the seismic hazard integral

$$P(A > Ao) = \sum_I \alpha_I \int_M \int_R f_I(M)\, f_I(R)\, P(A>Ao \mid M,R)\, dR\, dM, \qquad (1)$$

where A is a ground-motion parameter (i.e., peak ground acceleration, PGA, or spectral acceleration, Sa), Ao is the ground motion level to be exceeded, α_I is the annual rate of occurrence of the ith source, M is magnitude, R is distance, $f_I(M)$ is the probability density distribution of earthquake magnitude of the ith source, and $f_I(R)$ is the probability density distribution of distance from the ith source. Originally, hazard at a site (grid point) is calculated by applying the appropriate site amplification distribution P(As | Ar) to the ground-motion attenuation relations within the hazard integral so as to alter them to site-specific attenuation relations (Cramer, 2003, 2005). Thus, in equation 1, A = As and P(A>Ao | M,R) becomes P(As>Ao | M,R) for a soil site, and

$$P(As>Ao \mid M,R) = 1 - \int_{Ar} P(As \le Ao \mid Ar)\, P(Ar \mid M,R), \qquad (2)$$

where

$$P(As \le Ao \mid Ar) = \int_{As:-\infty \to Ao} P(As = Ao \mid Ar)\, dA \qquad (3)$$

and

$$P(Ar \mid M,R) = d[1 - P(A > Ar \mid M,R)] / dA. \qquad (4)$$

Basically, the site amplification distribution alters the rock hazard curve to a soil hazard curve for each earthquake in the hazard model before they are summed into the final soil hazard curve.

Lee (2000) has shown that instead of modifying the hazard curve of each earthquake in the hazard model and summing the resulting site-specific hazard curves to obtain the total site-specific hazard curve, the total hazard curve from the hard-rock hazard calculation can be modified directly by the site amplification distribution to make it site-specific:

$$P(As > Ao) = 1 - \int_{Ar} P(As \le Ao \mid Ar)\, P(Ar), \qquad (5)$$

where P(As ≤ Ao | Ar) is given by equation 2, and P(Ar) is from the total hard rock hazard curve and is given by

$$P(Ar) = d[1 - P(Ar > A)] / dA. \qquad (6)$$

This can be done because the site amplification distribution is explicitly independent of earthquake magnitude and distance and thus can be pulled outside of the seismic hazard integral (equation 1). It may seem that nonlinearity in soil response is implicitly dependent on magnitude and distance, but engineering models of nonlinear response are only dependent on the input level

of ground motion. Further, the nature of the total hazard curve emphasizes that the strong ground motions come from the nearest, largest earthquakes and hence nonlinear soil behavior is a function of ground-shaking strength. Comparisons between the inside-the-integral and outside-the-integral approaches at the Savannah River Site indicate that both approaches yield essentially the same hazard result (Lee, 2006, personal communication) and tests have shown a greater than 5 times savings in computational time for the outside-the-integral approach (Cramer, 2011). Additionally, even if the hazard estimate is from predominant earthquakes with differing distances for differing magnitude ranges that have varying site response among the magnitude ranges (but the same within a magnitude range), the outside-the-integral approach can be applied separately to each magnitude range and the resulting hazard curves for each magnitude range combined (Cramer, 2014).

Implementing this seismic hazard mapping methodology requires the development of a 3D geological and geotechnical model plus reference or grid-specific Vs profiles (Cramer et al., 2004, 2006). Via a Monte Carlo randomization procedure, site amplification distributions are developed at each grid point for each ground motion period for which hazard maps are developed (usually peak ground acceleration and 0.2, 0.3, and 1.0 s spectral acceleration). This can be accomplished using an equivalent linear or nonlinear soil response program. The choice of program is dependent on soil type and conditions (saturated or not), how far the study area is from seismic sources, and the expected ground motions from those sources as discussed above for the Charleston case (nonlinear possibly with dynamic pore-pressure effects). These site amplification distributions are relative to bedrock (hard rock conditions). The CAEHMP Community Velocity Model (CAEHMP major task 1; grant G16AP00025) provided the database of geological, water well, and geotechnical borings and geophysical measurements that allow for the implementation of this methodology. This methodology provides more realistic ground motion and liquefaction hazard estimates than the common engineering practice of using NEHRP site amplification factors that are incorporated into building codes. Loss estimates based on these improved ground motion estimates should also be more realistic.

Seismic hazard maps with the effect of local geology are the basis for generating liquefaction hazard maps (CAEHMP major task 4). To generate probabilistic liquefaction hazard maps, the final CAEHMP PGA seismic hazard maps and associated data are incorporated using the approach of Cramer et al. (2008), which was developed for the Memphis urban hazard-mapping project. Note that the liquefaction cumulative probability curves (from CAEHMP task 2) are a function of magnitude and hence are used inside the hazard integral to calculate probabilistic liquefaction hazard maps as indicated in the following equation from Cramer et al. (2008):

$$P(P_{LPI>n} > Po) = \Sigma_i \alpha_i \int_M \int_R f_i(M)\, f_i(R)\, P(P_{LPI>n} > Po \mid A>Ao,M)\, P(A>Ao \mid M,R)\, dR\, dM \quad (7)$$

where $P(P_{LPI>n} > Po)$ is the liquefaction hazard curve for LPI>n, α_i is the rate of source i, M and R are magnitude and distance, $f_i(M)$ and $f_i(R)$ are the ith source magnitude and distance distribution functions, $P(P_{LPI>n} > Po \mid A > Ao,M)$ is the liquefaction cumulative probability curve for the site and LPI>n, and $P(A > Ao \mid M,R)$ is the site-specific attenuation relation. Figure 7 shows how the various geological, seismological, and geotechnical elements are brought together to produce liquefaction hazard maps. The generation of final liquefaction hazard maps requires

the use of a GIS, guided by the surface geology map, to piece together liquefaction hazard maps for each surface soil type into a scenario or probabilistic liquefaction hazard map.

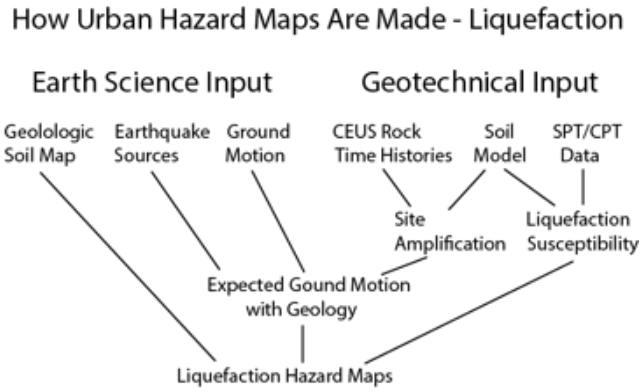

Figure 7: How urban seismic hazard maps are made - liquefaction

GMICE can be used to convert intensities to ground motions for comparison to scenario seismic hazard maps. For CENA, the latest published GMICE is Ogweno and Cramer (2017). Ogweno and Cramer (2017) is limited to modified Mercalli intensities (MMIs) VI and less because the low rate of CENA seismicity had not produced intensity/ground motion pair observations above MMI VI, with one exception. The recent Cushing, OK M5.0 earthquake provided good close-in ground motion observations for intensities VII and VIII, so we have just completed updating the Ogweno and Cramer (2017) GMICE to include intensities up to IX (Cramer, 2020). Above intensity IV, the rate of ground motion increase with increased intensity is reduce (Figure 8). MMI VI and below is dominated by observations of ground motion on people and small objects; above MMI VI they are dominated by damage to structures. This results in the commonly observed change in the slope of ground motion increase at about MMI V. Now that we have CENA observations above VI we have updated relations to IX to evaluate the effects of alternative 1886 source models and compare them to ground motions from converted 1886 intensities. Then probabilities can better be assigned to alternative 1886 source models and used in a probabilistic evaluation for use in probabilistic seismic hazard analyses. There are three alternative source models for the 1886 Charleston earthquake: Dura-Gomez and Talwani (2009) with a vertical fault with offset ~35 km from downtown Charleston, Chapman et al. (2016) with a westward dipping fault ~35 km away, and Pratt et al. (2014) with a vertical fault at 35 km from Charleston. We evaluated all three source models using scenario seismic hazard maps with the effects of local geology and the MMI X zone of Bollinger (1977) in order to evaluate the likelihood of each source model being responsible for the 1886 M7.0 Charleston, SC earthquake.

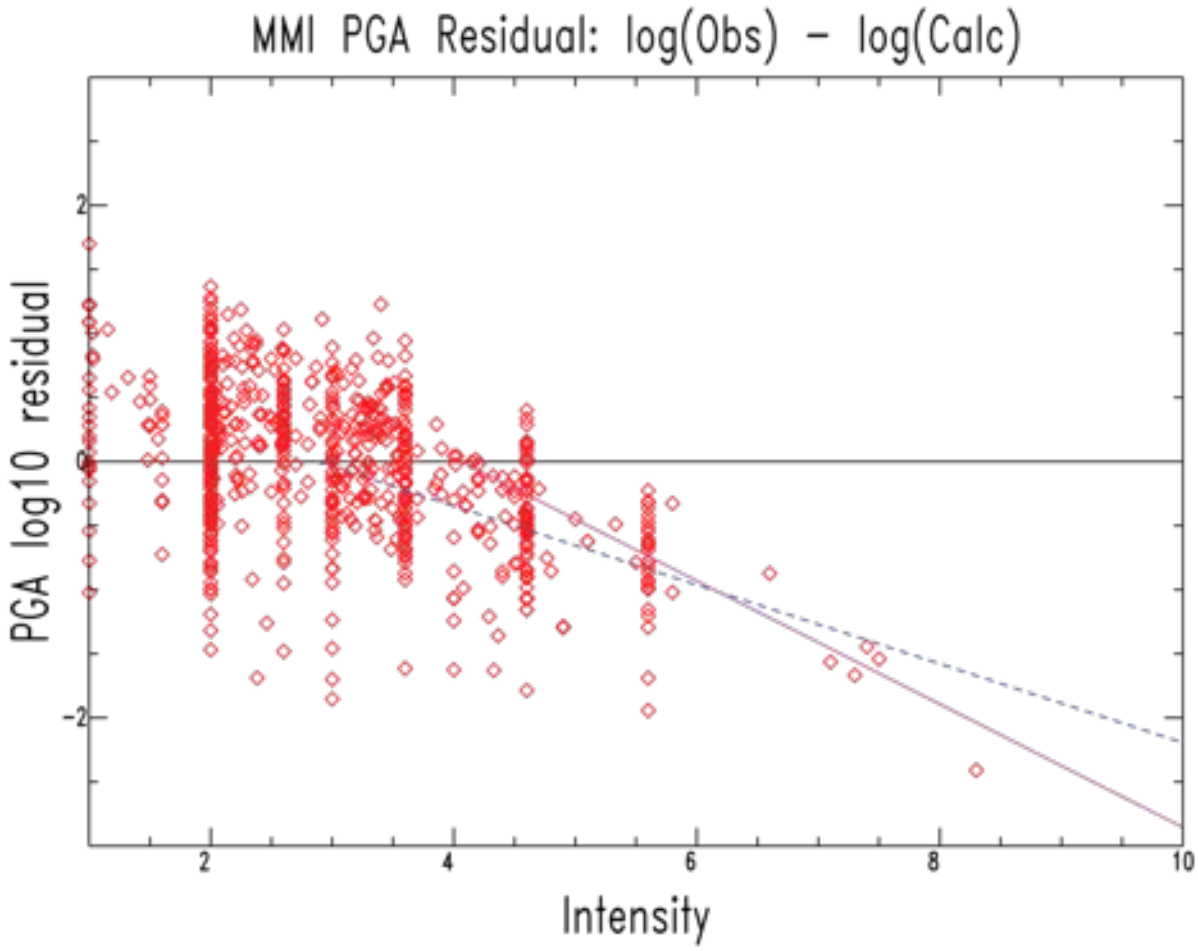

Figure 8: GMICE data and linear trend used to update Ogweno and Cramer (2017) for use above MMI VI. Log PGA residuals below IV cluster around zero, but deviate to the slope shown above IV. Fits to intensity five and greater (solid magenta) and four and greater (dashed blue) are shown. The solid line has the minimum standard deviation and best represents the trend above MMI IV.

Updated Charleston Quadrangle Surface Geology

During the course of the initial pilot project (Jaumé et al., 2015, 2016) and Community Velocity Model development (Jaumé and Levine, 2018) in became clear that human modification of the land surface (particularly the addition of artificial fill) effectively hid geotechnically important material boundaries, and that much of this modification occurred before the advent of modern geological mapping (Weems et al., 2014 and references therein). Based upon feedback from the Charleston area geotechnical community (B. Camp, M. Ulmer and G. Canivan, pers. comm.), the 1949 Halsey Map (http://halseymap.com) of Charleston is considered to be the best representation of the pre-modification dry land/tidal marsh boundary of the Charleston peninsula. The Halsey Map was compiled by a City of Charleston engineer Alfred O. Halsey based upon multiple historical sources, and Alfred O. Halsey superimposed the dry land/tidal marsh boundary plus additional historical features upon a 1946 City Engineers Map of the City of Charleston.

Recent studies of flooding on the Charleston peninsula (e.g., Dutch Dialogues Charleston https://www.dutchdialoguescharleston.org/) found a strong correlation between former tidal marsh areas on the Halsey Map and current low elevation locations subject to repeated flooding. We also compiled information from multiple geotechnical reports within the area covered by the Halsey Map and determined that substantial portions of the current USGS surficial geology map (Weems et al., 2014) misrepresent seismic site conditions on the Charleston quadrangle (Jaumé et al., 2019); in particular areas mapped as artificial fill (af) can cover both extremely low Vs (50-100 m/sec) Holocene tidal marsh (Qht) as well as the higher Vs (180-190 m/sec) Silver Bluff (Qsb) & Wando (Qw) formations. Thus, with the concurrence of members of the stakeholders group that participated in the July 2019 workshop, we decided to undertake a "remapping" of the Charleston quadrangle surface geology in order to better represent seismic site conditions there.

With assistance from personnel from the College of Charleston Addlestone Library, we scanned and georectified the Halsey Map, then digitized the tidal marsh boundary from the high-resolution scan. We also obtained the 1911 USGS topographic map of the Charleston quadrangle, georectified it and digitized the tidal marsh boundary on that map to complement the Halsey Map tidal marsh boundary. Both tidal marsh boundaries where then compared to high-resolution LiDAR digital elevation models (DEM) of the Charleston quadrangle. We found that the tidal marsh boundary of the Halsey Map closely corresponds to the 7.3 to 7.5 -foot elevation contours on the DEM. A similar correlation occurs in many areas outside downtown Charleston using the tidal marsh boundary from the 1911 topographic map. This elevation contour was then digitized, and those areas below 7.5 and above 7.3 feet where designated either as either artificial fill (af) or Holocene tidal marsh (Qht) based the overall correspondence of the 1911 marsh boundaries with the current Lidar based digital elevation model. Those areas previously designated af that lay above the 7.7 foot contour where assigned the same surface geology (in most cases a facies of either the Silver Bluff (Qsb) or Wando (Qw) formations) as the nearest surface geology unit.

Figure 9 shows a side by side comparison of the surface geology as mapped by Weems et al., 2014 versus our update. In most cases the changes have a minor impact on the 9 quadrangle (~500 m spacing) seismic and liquefaction hazard maps but are much more substantial on the more detailed (~100 m spacing) maps of the Charleston quadrangle.

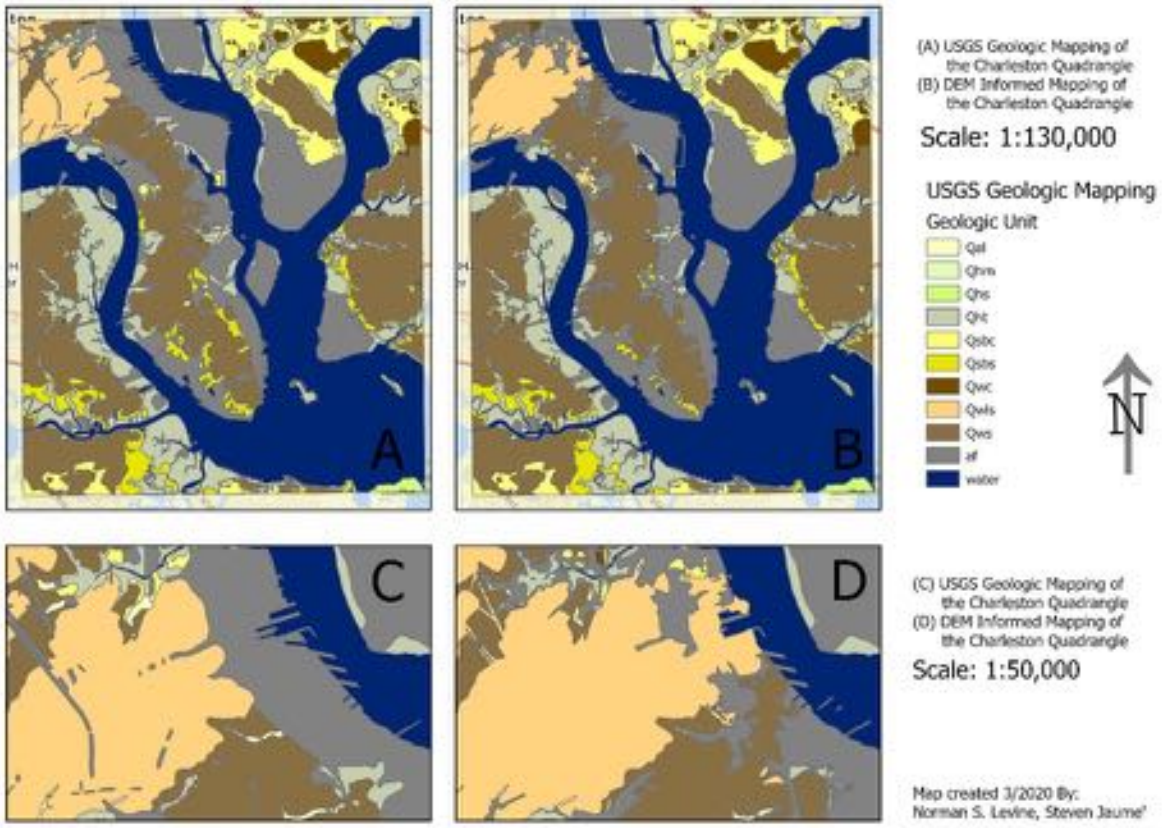

Figure 9: Left: Original (Weens et al., 2014) surface geology map of the Charleston quadrangle. Right: Our revised surface geology map based upon the 1949 Halsey Map, 1911 USGS topographic map and 7.3 foot DEM contour.

Hazard Maps

The base seismic hazard model used in this study is the 2014 USGS national seismic hazard source and attenuation models (Petersen et al., 2014). The recently released 2018 USGS model (Petersen et al., 2019) was officially released in December of 2019, too late for use in this study. The effects of local geology were added to the 2014 model and seismic and liquefaction hazard maps generated as described in the Methodology section above. Petersen et al. (2019) state that the 2018 national maps are generally higher than the 2014 national maps (up to ~ 30%). But the nonlinear soil behavior in the Charleston area will counter this increase in ground motion. Experience in the Mississippi embayment (similar geological setting at the Coastal Plain around Charleston) shows that for strong ground motions in thick, soft sediments the nonlinear soil effects balance out the increase (or decrease) in rock ground motion to the point where seismic hazard estimates are very similar on soft soils. Thus, we expect that the Charleston Area

Earthquake Hazards Mapping Project (CAEHMP) seismic and liquefaction hazard results will be essentially the same using the 2014 or 2018 USGS national seismic hazard model.

Caveats: The hazard maps presented in this report are still regional in nature and not site-specific hazard maps. While they can provide guidance for site-specific studies, they are NOT site-specific hazard maps as such. These hazard maps are still regional in nature due to the relatively sparse coverage of the geologic information that comprises the community velocity (3D geology) model used in this study. If a site-specific study is desired at a specific location, site-specific geological, geotechnical, and geophysics data should be used from that specific site. Further, while artificial fill has been mapped and hazard estimates provided, sites on artificial fill should be considered within a "special study zone" and a true site-specific study required for engineering design purposes.

Seismic Hazard Maps

We produced both probabilistic and scenario (deterministic) seismic hazard maps for the nine-quadrangle study area on a ~500-meter grid. Additionally, for the Charleston quadrangle only, we produced the same hazard maps on a ~100-meter grid. The data available in the community velocity model was sufficiently dense to warrant producing hazard maps at a higher resolution for this one quadrangle.

Seismic hazard maps were produced for the following periods: peak ground acceleration (PGA) and 0.1, 0.2, 0.3, 0.5, 1.0, and 2.0 s spectral acceleration (Sa). In this report we only show the PGA, 0.2s, and 1.0s maps. The other maps are available from the Lowcountry Hazard Center website (https://arcg.is/1nPWuy).

Probabilistic seismic hazard maps were generated at 2%-in-50y, 5%-in-50y, and 10%-in-50 y probability of exceedance. The 2%-in-50y probability of exceedance seismic hazard maps are the basis for building code engineering design. The 5%-in-50y probability of exceedance seismic hazard maps are similar to the median scenario seismic hazard maps for a M7 in the Charleston seismic zone like the 1886 M7.0 Charleston earthquake near Summerville (magnitude from Cramer and Boyd, 2014). We do not recommend the 10%-in-50y probability of exceedance hazard maps for engineering design as they are no longer acceptable by current building code standards.

Figure 10 presents the 2%-in-50y probability of exceedance hazard maps for the nine-quadrangle study area. In the background are the 2014 USGS seismic hazard maps for B/C boundary soil conditions (Vs30 of 760 m/s) for comparison. The CAEHMP PGA hazard maps for 2%-in-50y hazard ranges from 0.3 to 0.5 g and show an approximately 50% reduction from the 2014 USGS equivalent hazard maps. The CAEHMP 0.2 s maps range from 0.3 to 0.6 g and represent about a 70% reduction from the equivalent 2014 USGS maps. For 1.0 s, the CAEHMP maps range from 0.3 to 0.4 g with a 20% reduction to a 30% increase relative to the equivalent 2014 USGS hazard map.

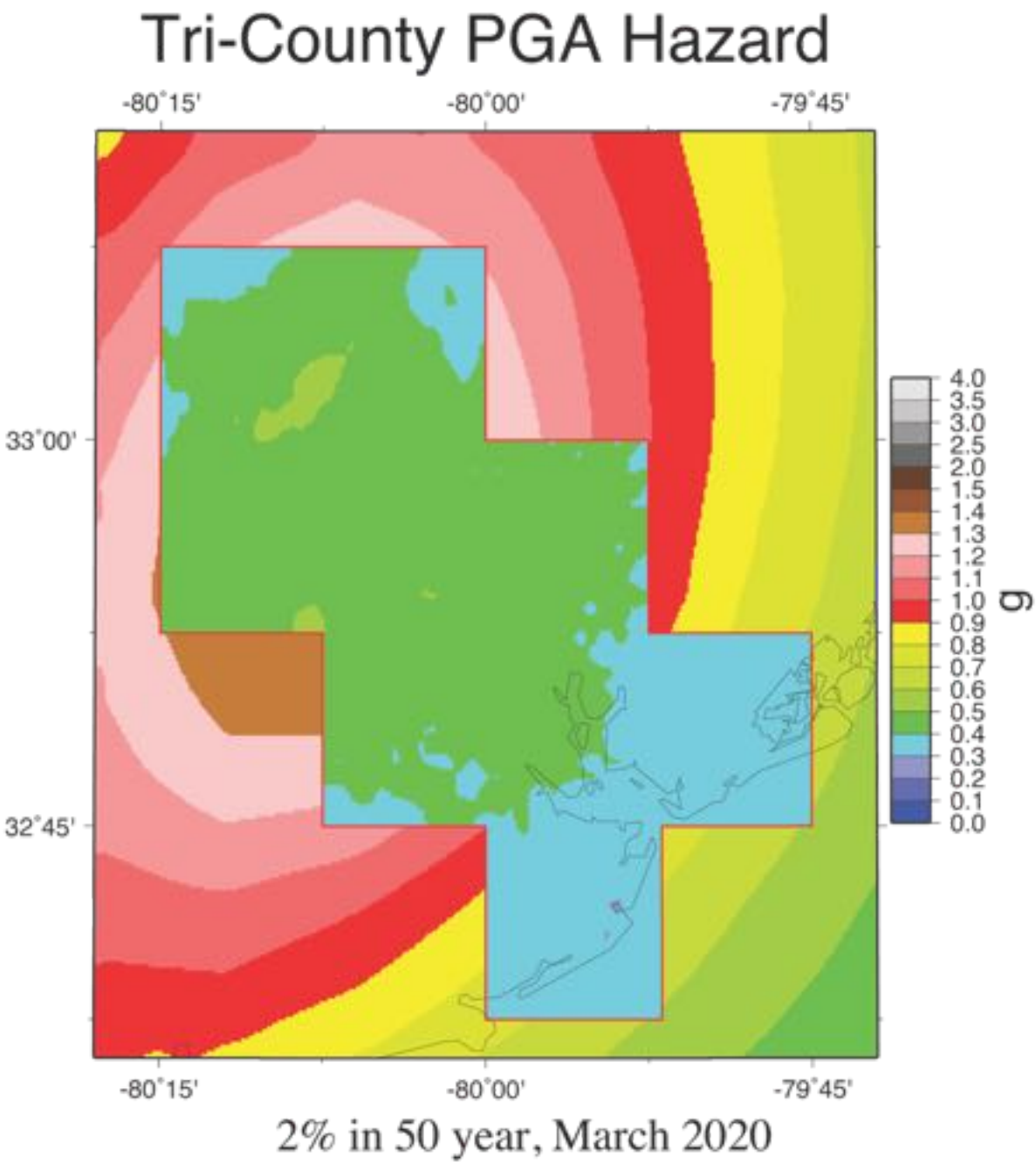

Figure 10a: PGA probabilistic seismic hazard map for all nine-quadrangles with the USGS 2014 B/C boundary national seismic hazard map in the background.

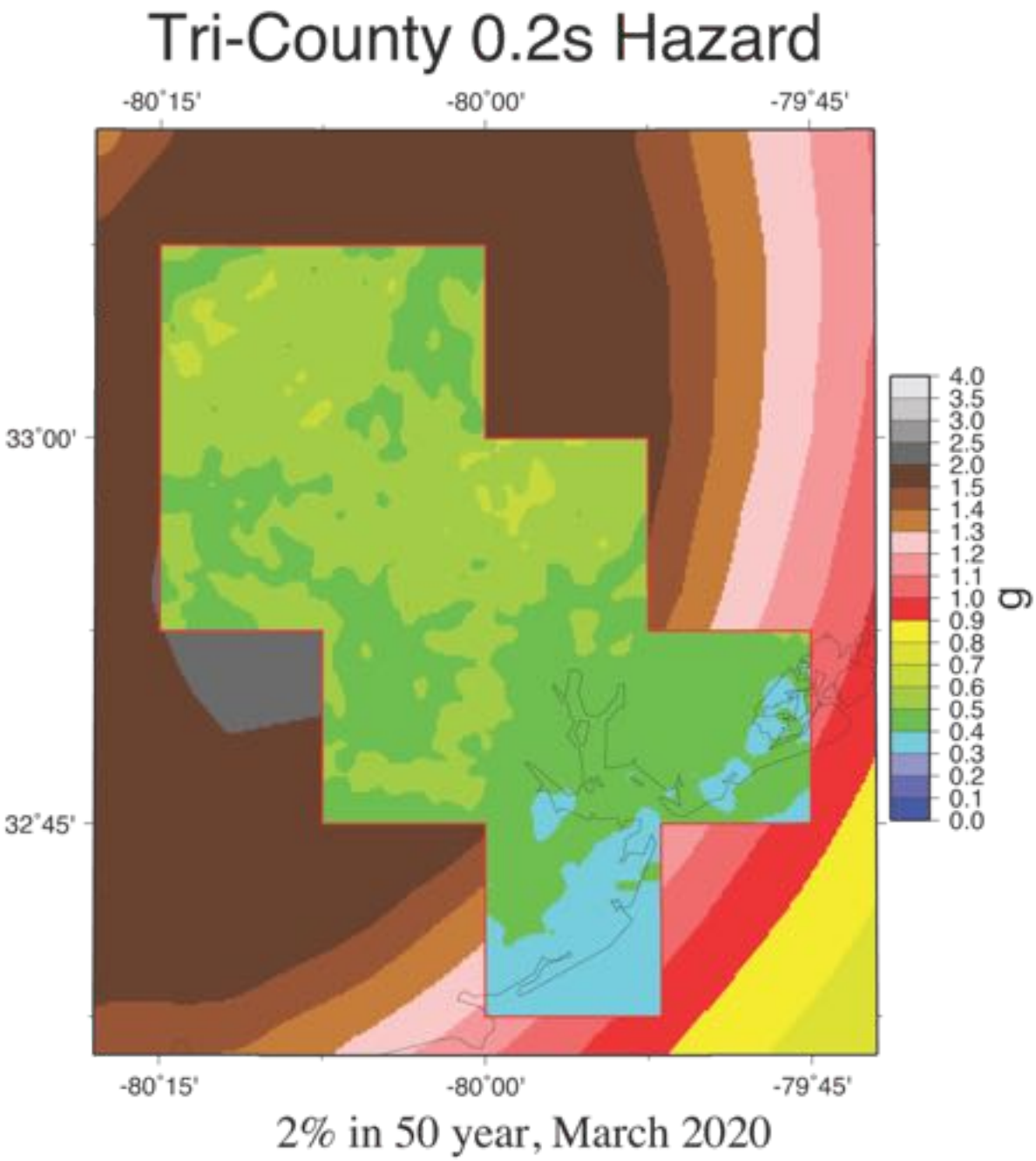

Figure 10b: 0.2 s probabilistic seismic hazard map for all nine-quadrangles with the USGS 2014 B/C boundary national seismic hazard map in the background.

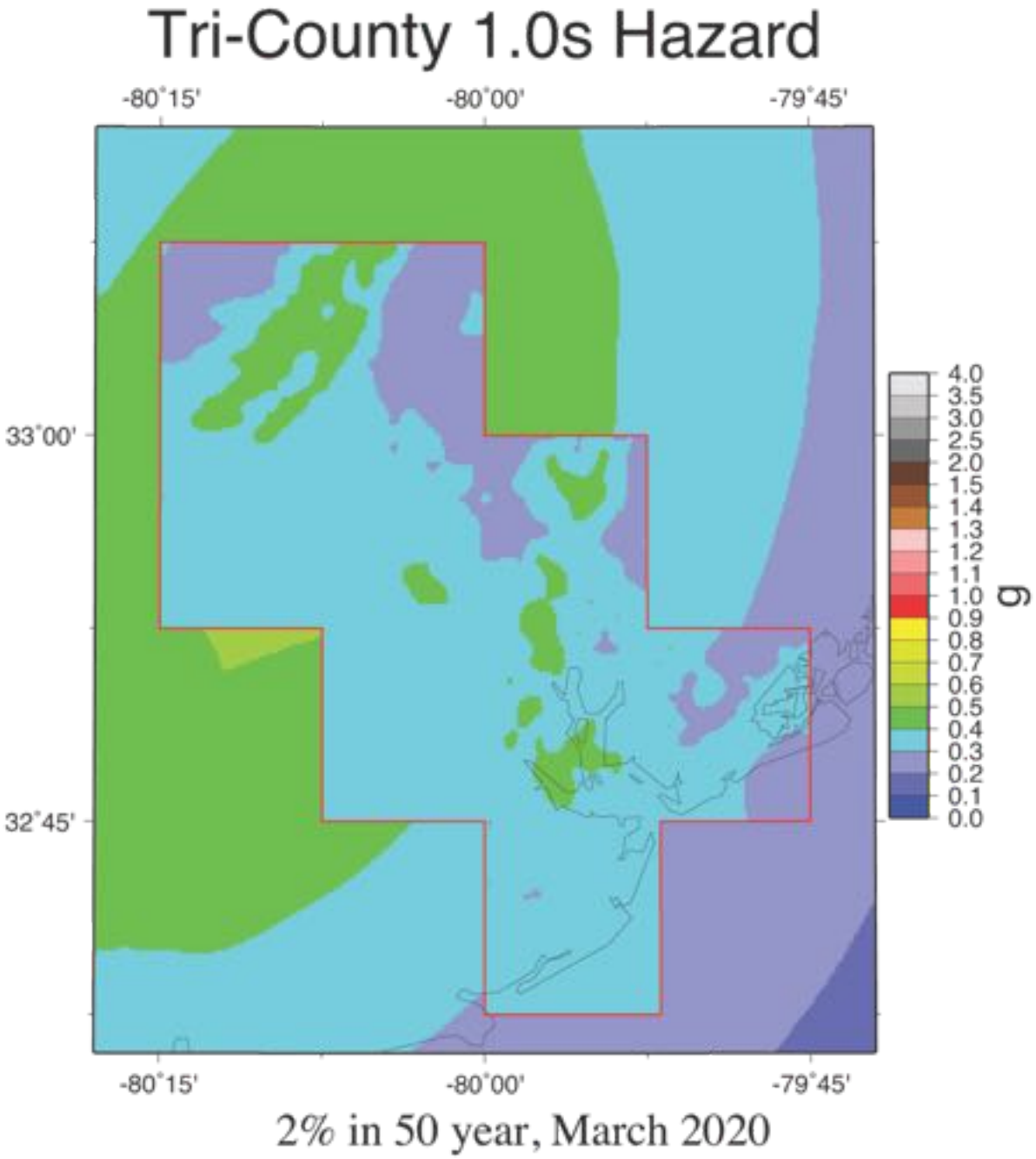

Figure 10c: 1.0 s probabilistic seismic hazard map for all nine-quadrangles with the USGS 2014 B/C boundary national seismic hazard map in the background.

Figure 11 presents the 2%-in-50y hazard maps for the Charleston quadrangle at higher resolution. In Figure 11 the ~100 m grid is more obvious, giving a more pixelated view. There is no comparison with the 2014 USGS equivalent B/C boundary maps in Figure 11, but the comparison from Figure 10 still holds.

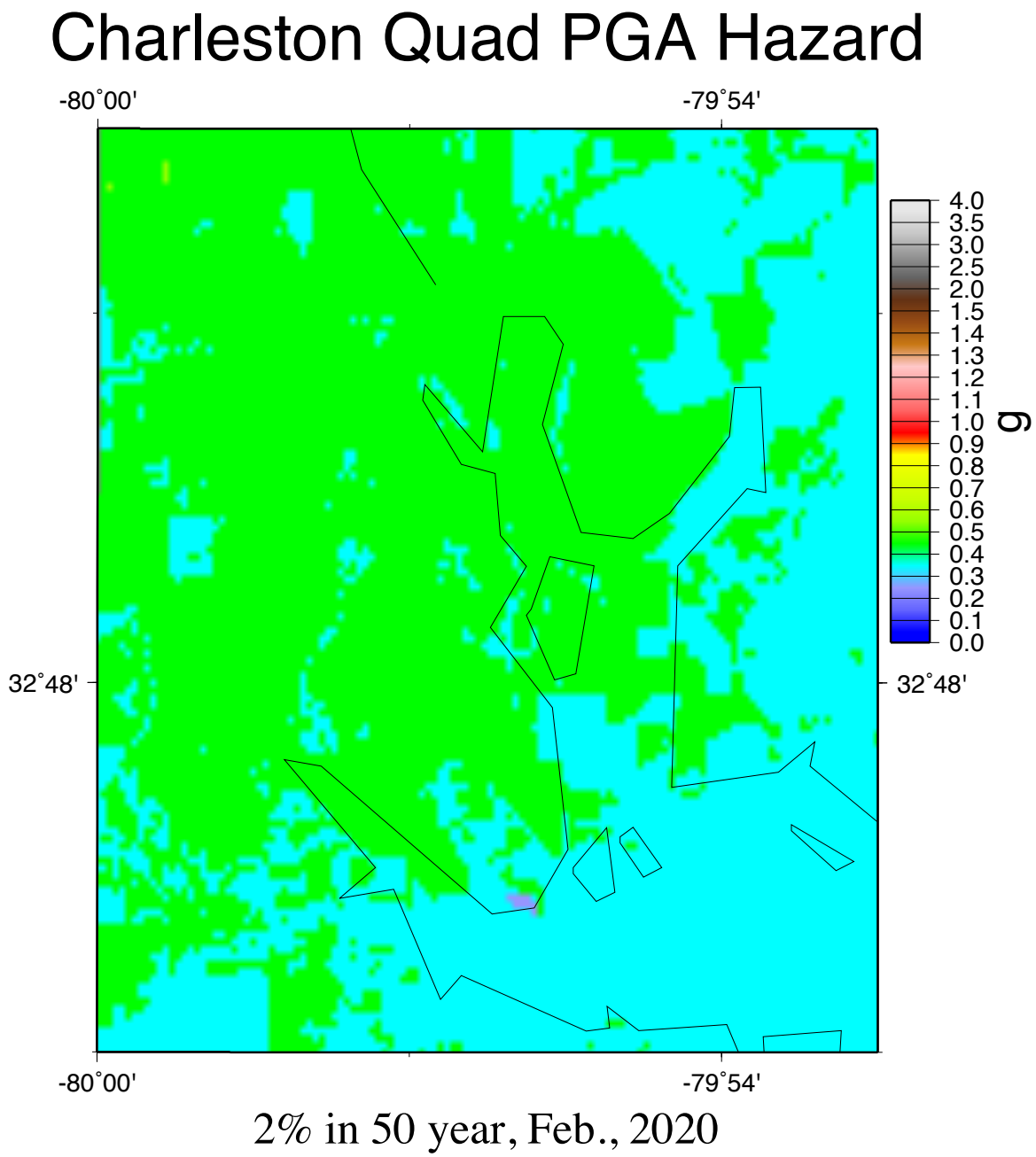

Figure 11a: Higher resolution PGA probabilistic seismic hazard map for the Charleston quadrangle.

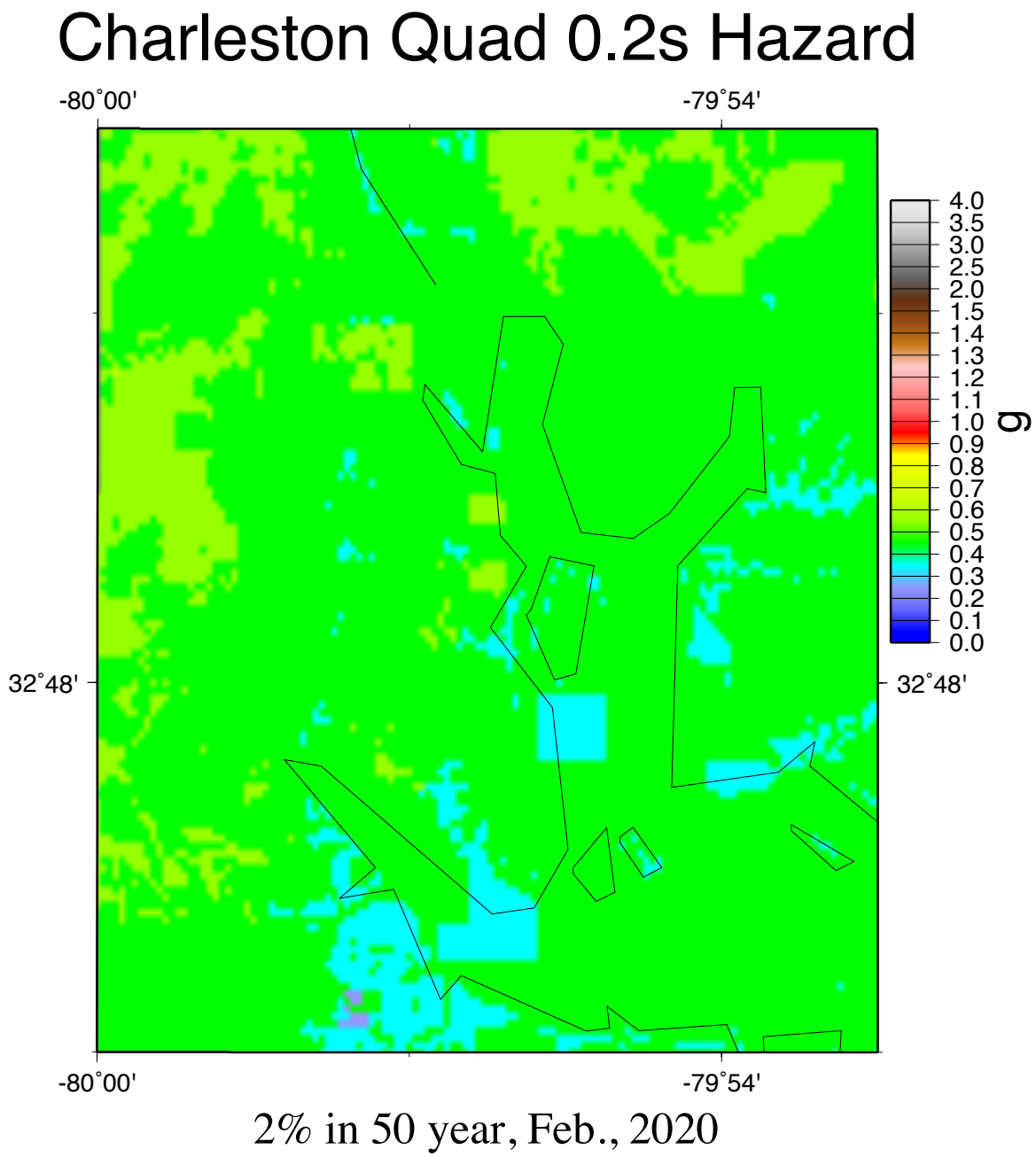

Figure 11b: Higher resolution 0.2 s probabilistic seismic hazard map for the Charleston quadrangle.

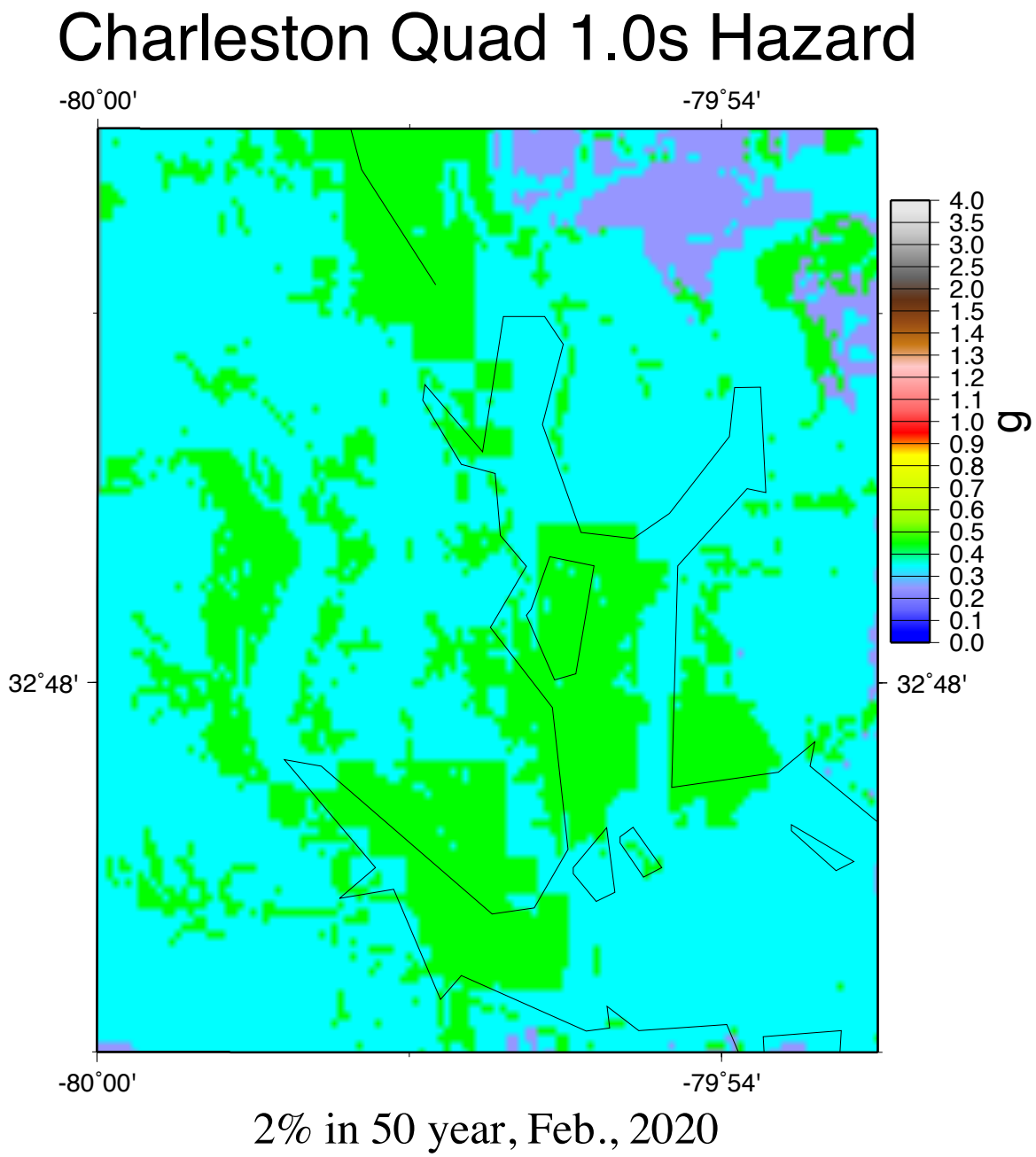

Figure 11c: Higher resolution 1.0 s probabilistic seismic hazard map for the Charleston quadrangle.

We also generated several scenario seismic hazard maps for several different scenarios and source regions. Figure 12 shows the basic three source regions used in this study: the Charleston seismic zone near Summerville, the offshore Edisto seismic area southeast of Charleston, and the St. George seismic area northwest of Charleston. For the Charleston seismic zone, which is the closest to Charleston, we generated scenario seismic hazard maps for M 5.0, 5.5, 6.0, 6.5, 7.0, and 7.3 at the request of our user community. For the offshore Edisto and St. George seismic source areas, we generated scenario seismic hazard maps for M 6.0, 6.5, and 7.0. Additional M7.0 scenario hazard maps were generated for the alternative 1886 source study as discussed later in the 1886 Alternative Source section.

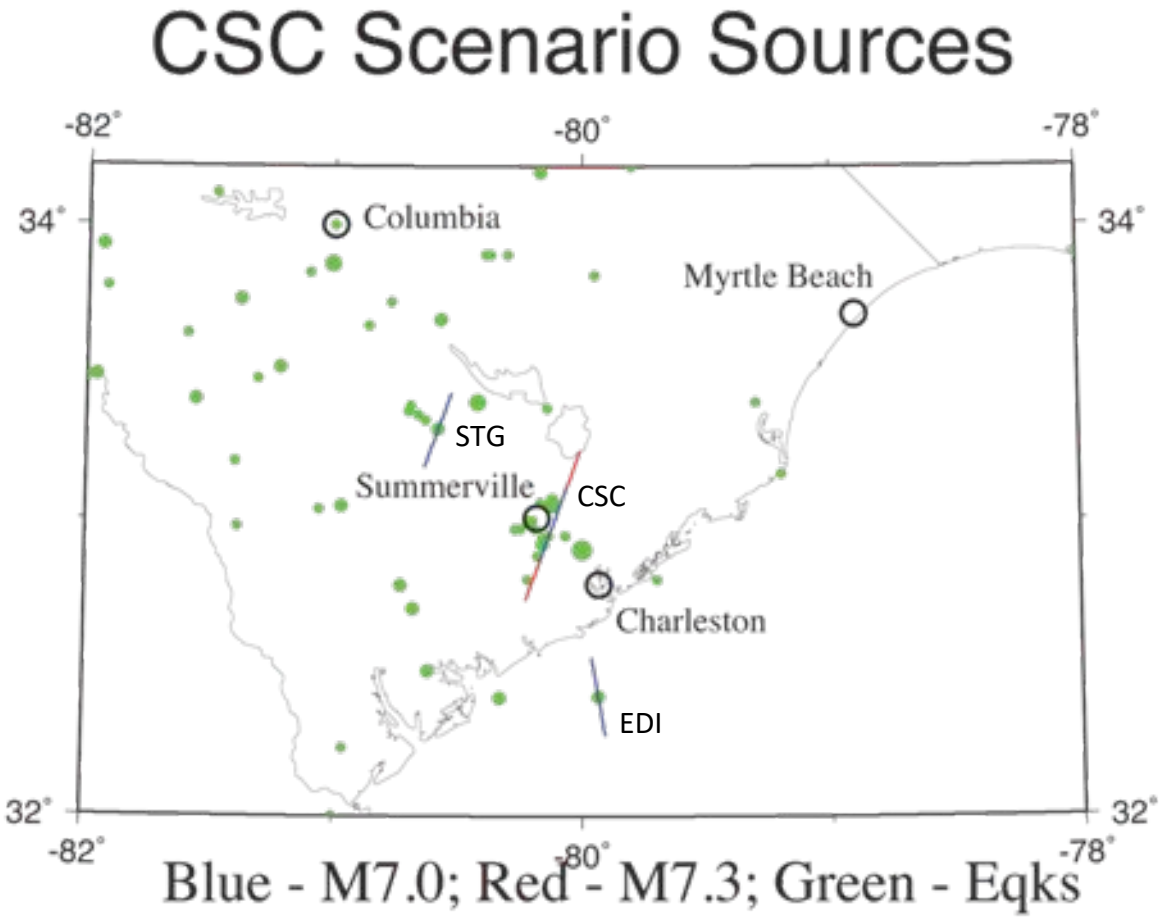

Figure 12: Map of source fault locations (lines) used to generate scenario hazard maps. CSC – Charleston seismic zone, EDI – offshore Edisto seismic area, and STG – St. George seismic area.

Figure 13 presents the M7.0 scenario seismic hazard maps for the Charleston seismic zone near Summerville. The ground motions are highest near the source (Summerville area). The PGA hazard ranges from 0.2 to 0.4 g, the 0.2s and 1.0s hazard from 0.2 to 0.3 g. Particularly for the 0.2 and 1.0 s hazard, the older beach sands, which are thicker Quaternary deposits show increased hazard, likely due to site resonance. Like the probabilistic hazard maps, these scenario hazard maps show similar ground motion levels at 0.2 and 1.0 s due to nonlinear soil effects at 0.2 s. Normally on rock, the 0.2 s ground motions are much higher than the 1.0 s ground

motions. Although not shown in this report, the hazard at 0.1, 0.3, 0.5, and 2.0 s and for all seven periods at magnitudes ranging from 5.0 to 6.5 in 0.5 magnitude steps are available at the Lowcountry Hazard Center website (https://arcg.is/1nPWuy).

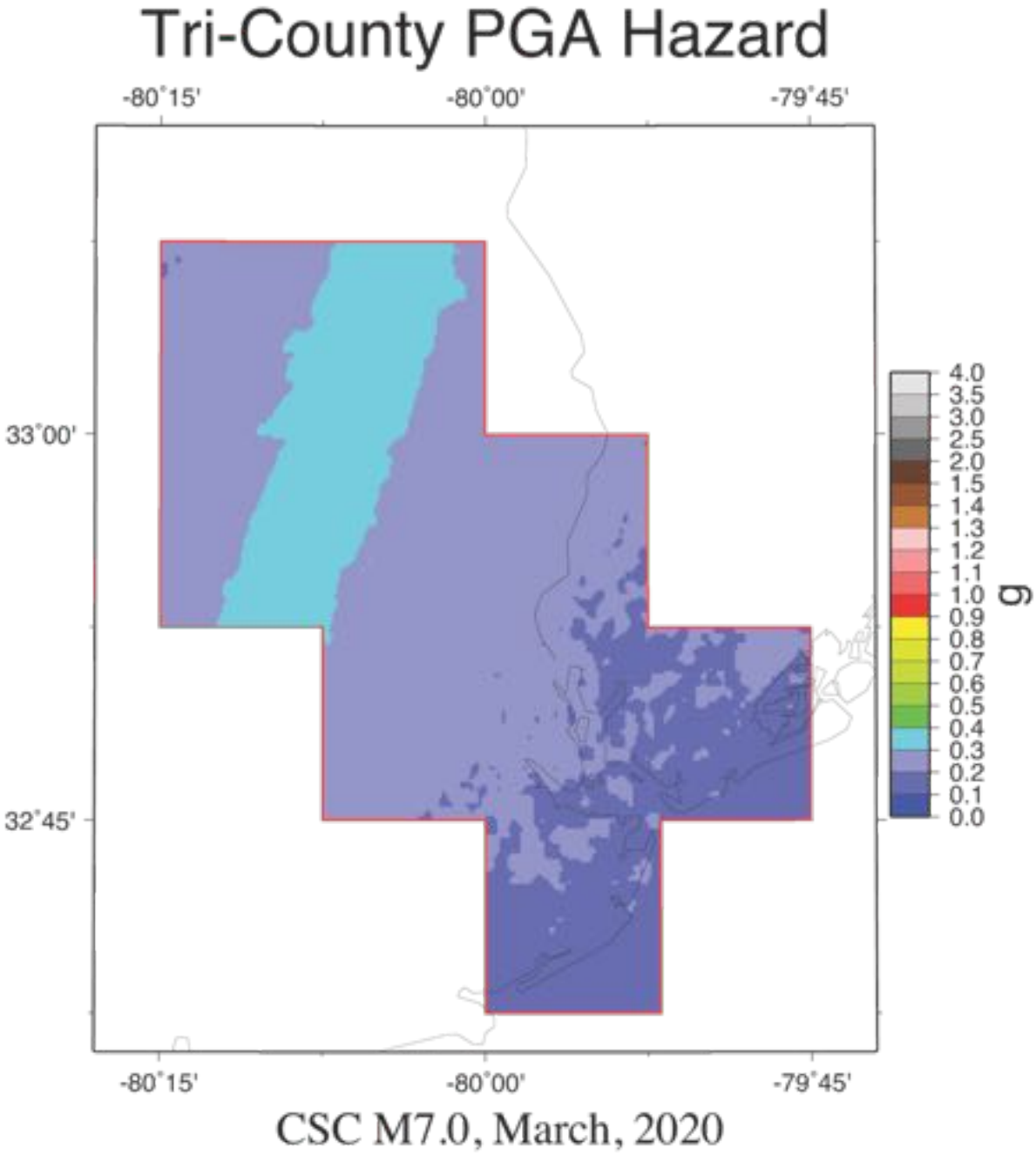

Figure 13a: PGA scenario seismic hazard map for all nine-quadrangles for a M7.0 in the Charleston seismic zone near Summerville.

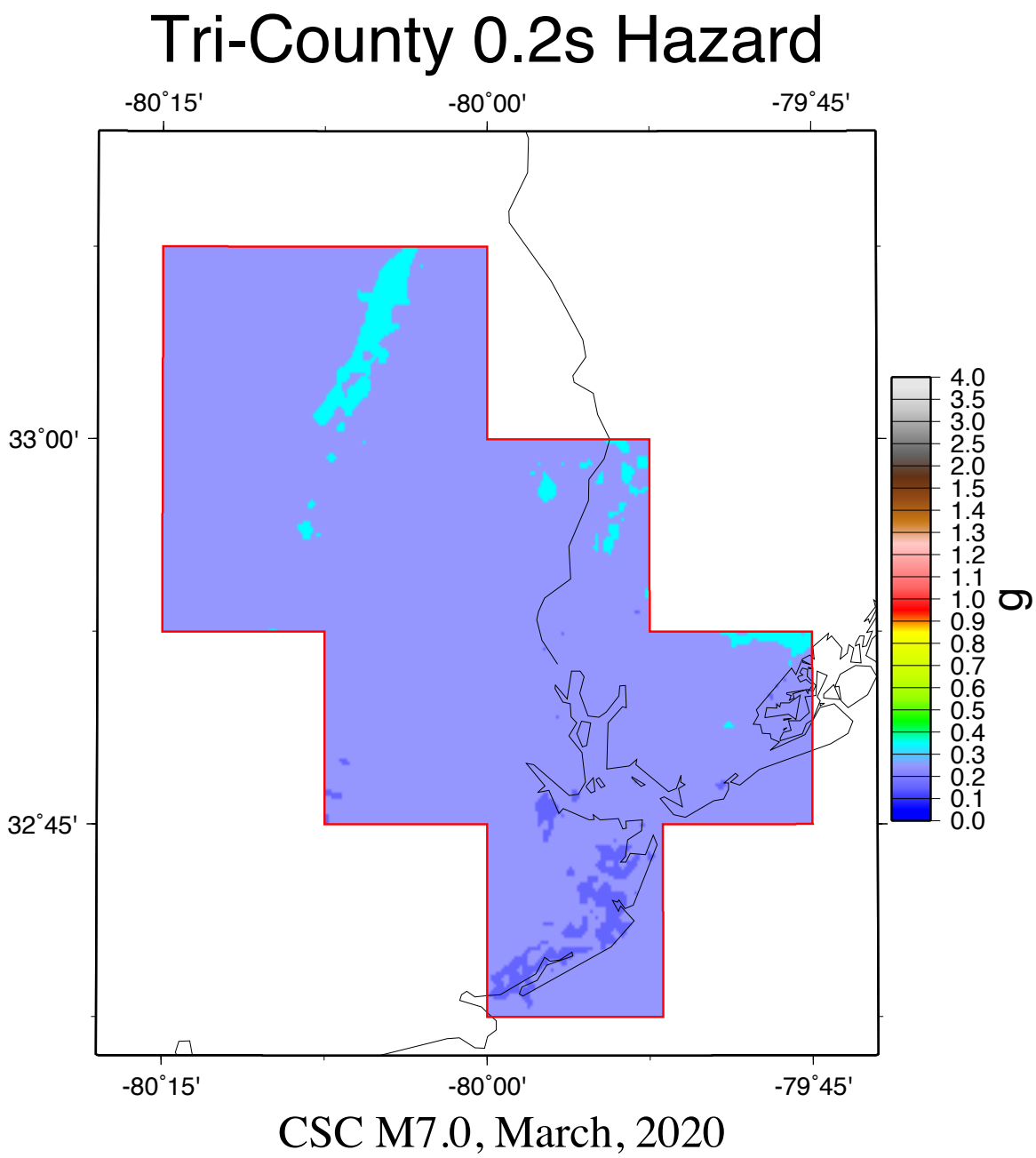

Figure 13b: 0.2 s scenario seismic hazard map for all nine-quadrangles for a M7.0 in the Charleston seismic zone near Summerville.

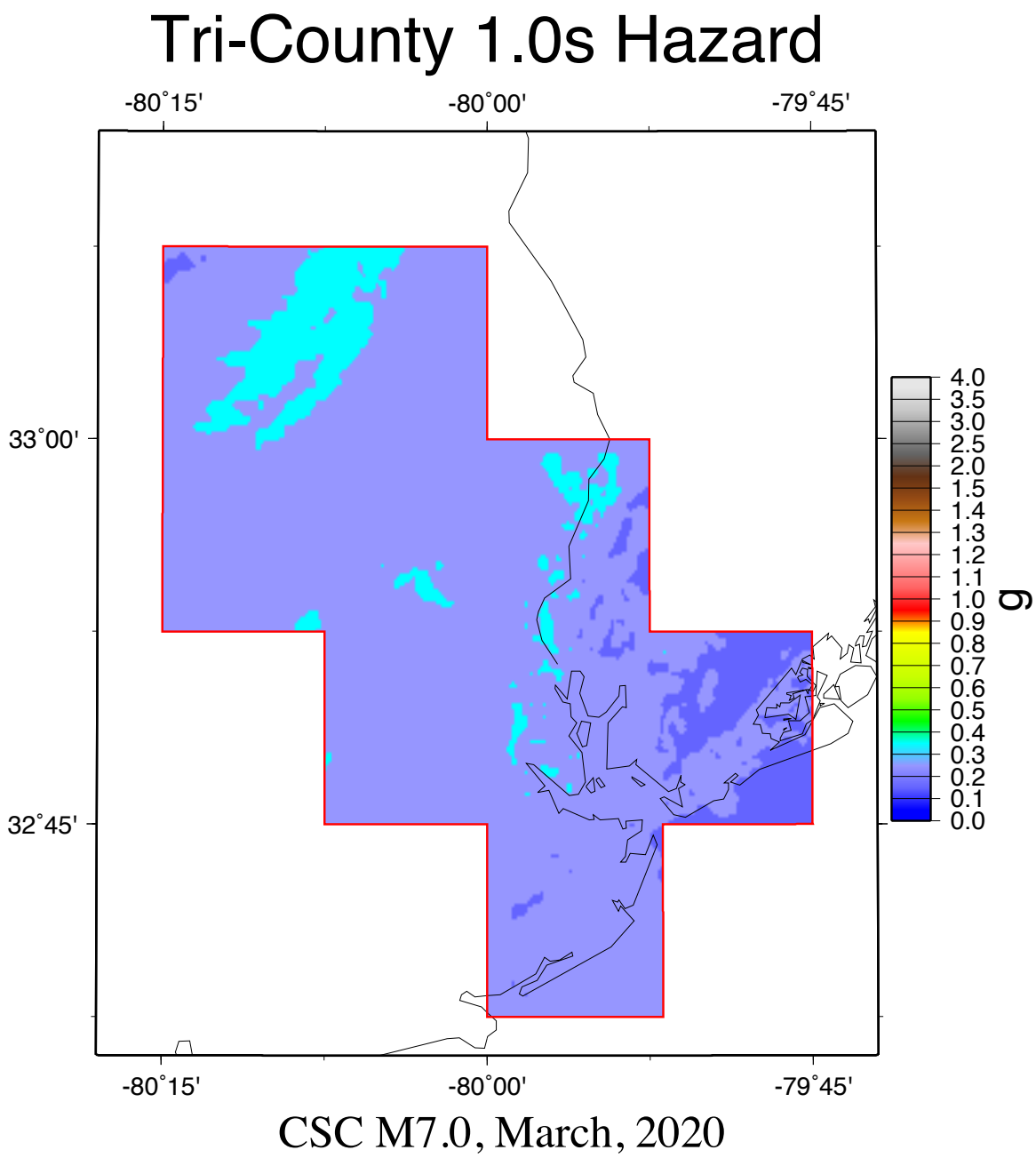

Figure 13c: 1.0 s scenario seismic hazard map for all nine-quadrangles for a M7.0 in the Charleston seismic zone near Summerville.

Figure 14 shows the M7.0 scenario seismic hazard from the Charleston seismic zone for the Charleston quadrangle in a manner similar to Figure 13 for the full nine-quadrangle study area only at the higher resolution of ~100 m. Ground motion levels are as in Figure 13. As in Figure 11, the ~100 m. grid is more obvious giving a more pixelated view.

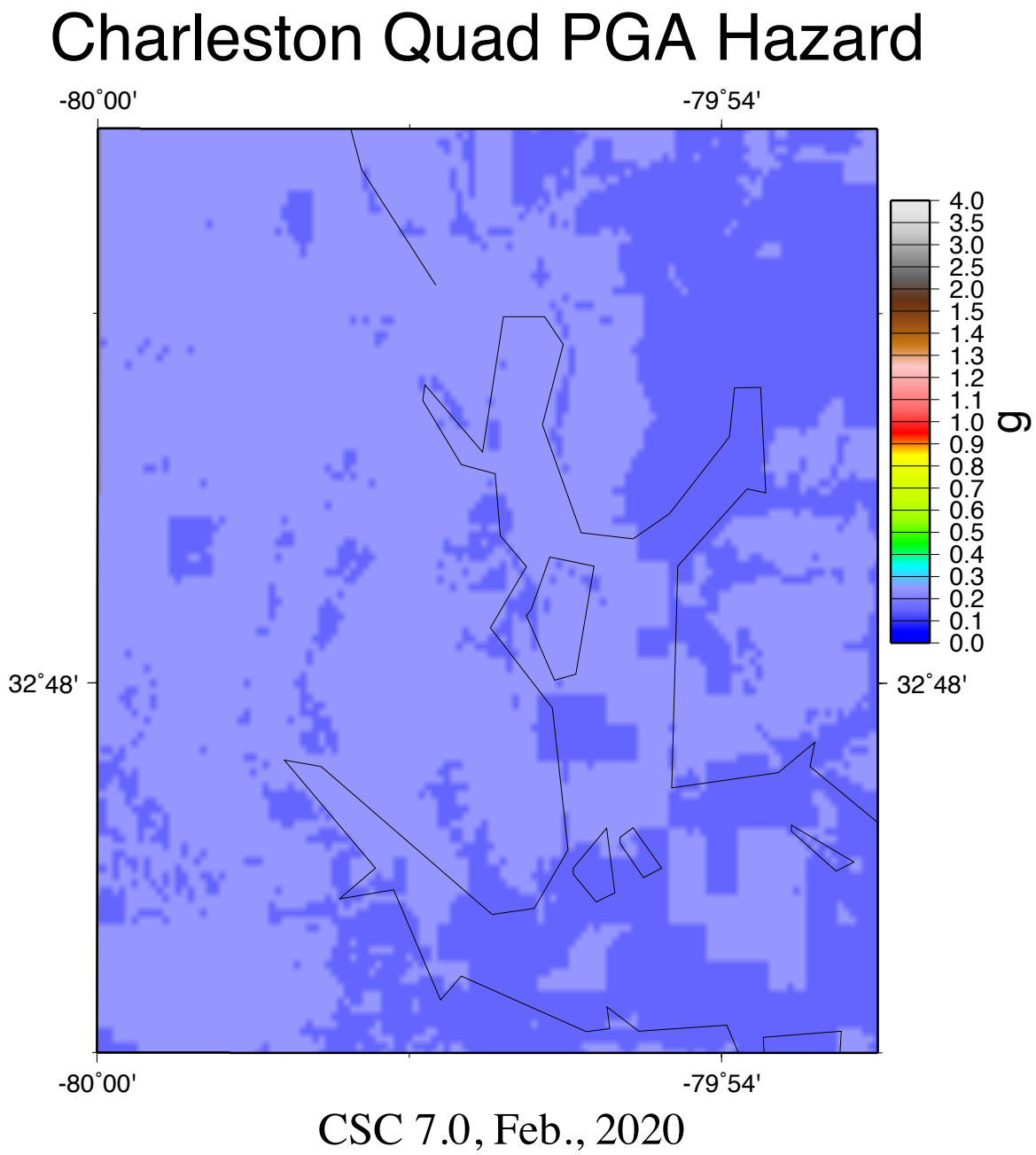

Figure 14a: Higher resolution PGA scenario seismic hazard map for the Charleston quadrangle for a M7.0 in the Charleston seismic zone near Summerville.

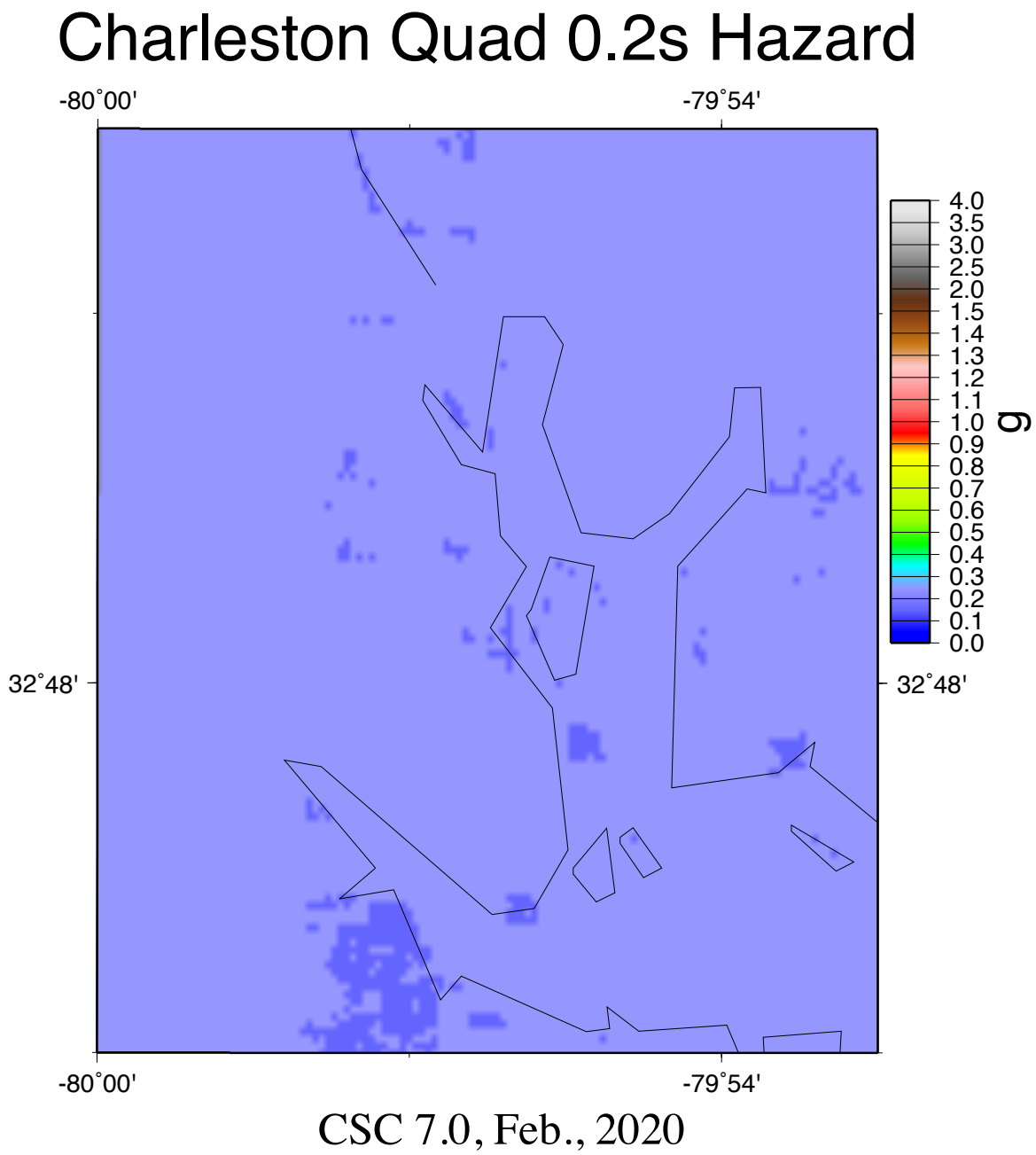

Figure 14b: Higher resolution 0.2 s scenario seismic hazard map for the Charleston quadrangle for a M7.0 in the Charleston seismic zone near Summerville.

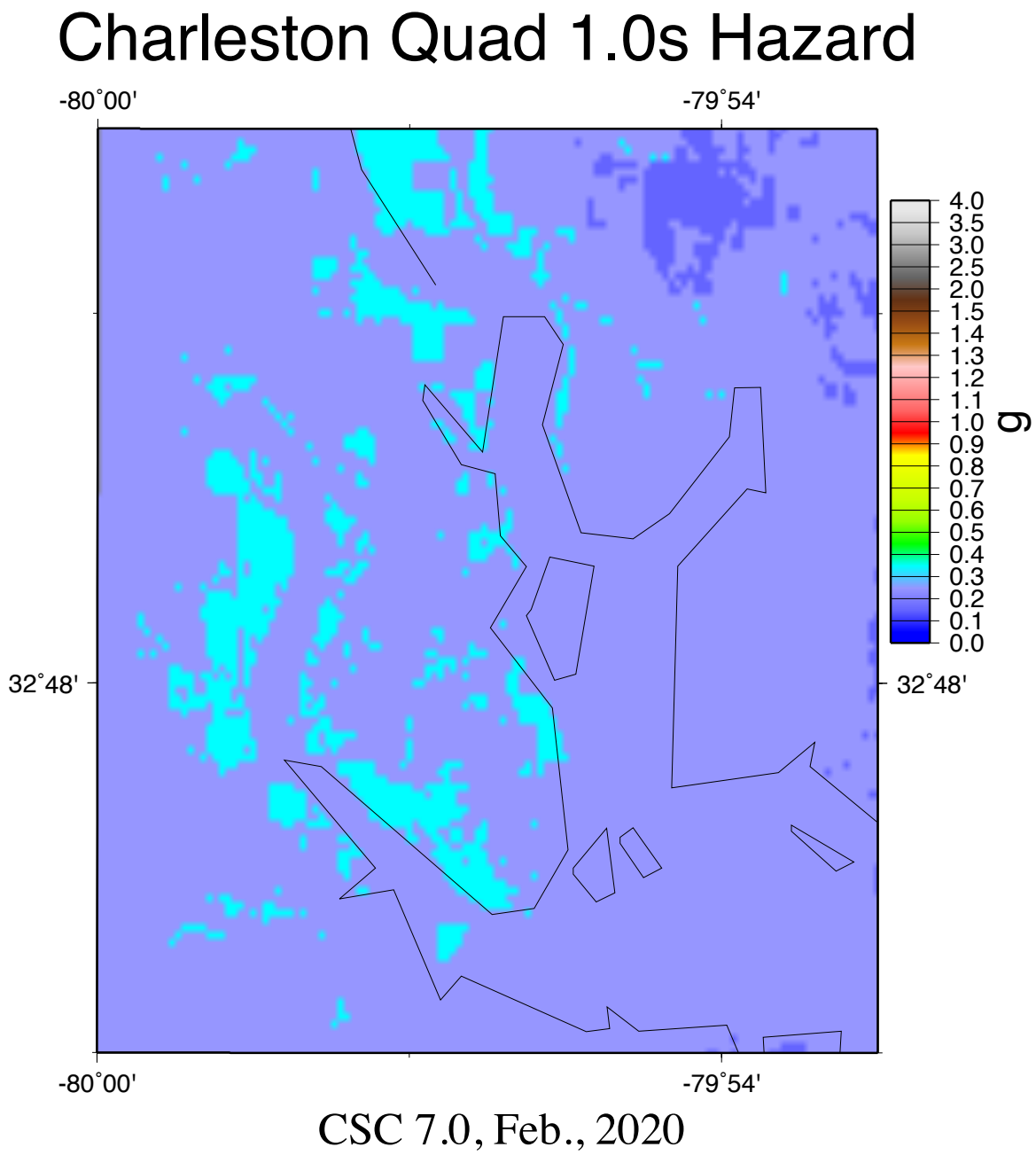

Figure 14c: Higher resolution 1.0 s scenario seismic hazard map for the Charleston quadrangle for a M7.0 in the Charleston seismic zone near Summerville.

Figures 15 and 16 present the M7.0 scenario seismic hazard maps from the offshore Edisto and St. George source areas, respectively. These source areas are about 50 km from Charleston, with the offshore Edisto source being somewhat closer than the St. George source. The PGA hazard for the nine-quadrangle study area ranges from 0.1 to 0.25 g for offshore Edisto and from 0.1 to 0.2 g for St. George. At 0.2s the ground motion ranges from 0.2 to 0.3 g for offshore Edisto and 0.1 to 0.3 g for St. George. And at 1.0 s the ranges are from 0.1 to 0.3 g for offshore Edisto and 0.1 to 0.2 g for St. George. These two sources still pose significant hazard to the Charleston area. The hazard maps for the magnitude 6.0 and 6.5 earthquakes for these two seismic sources along with hazard at the other four periods are available at the Lowcountry Hazard Center website (https://arcg.is/1nPWuy).

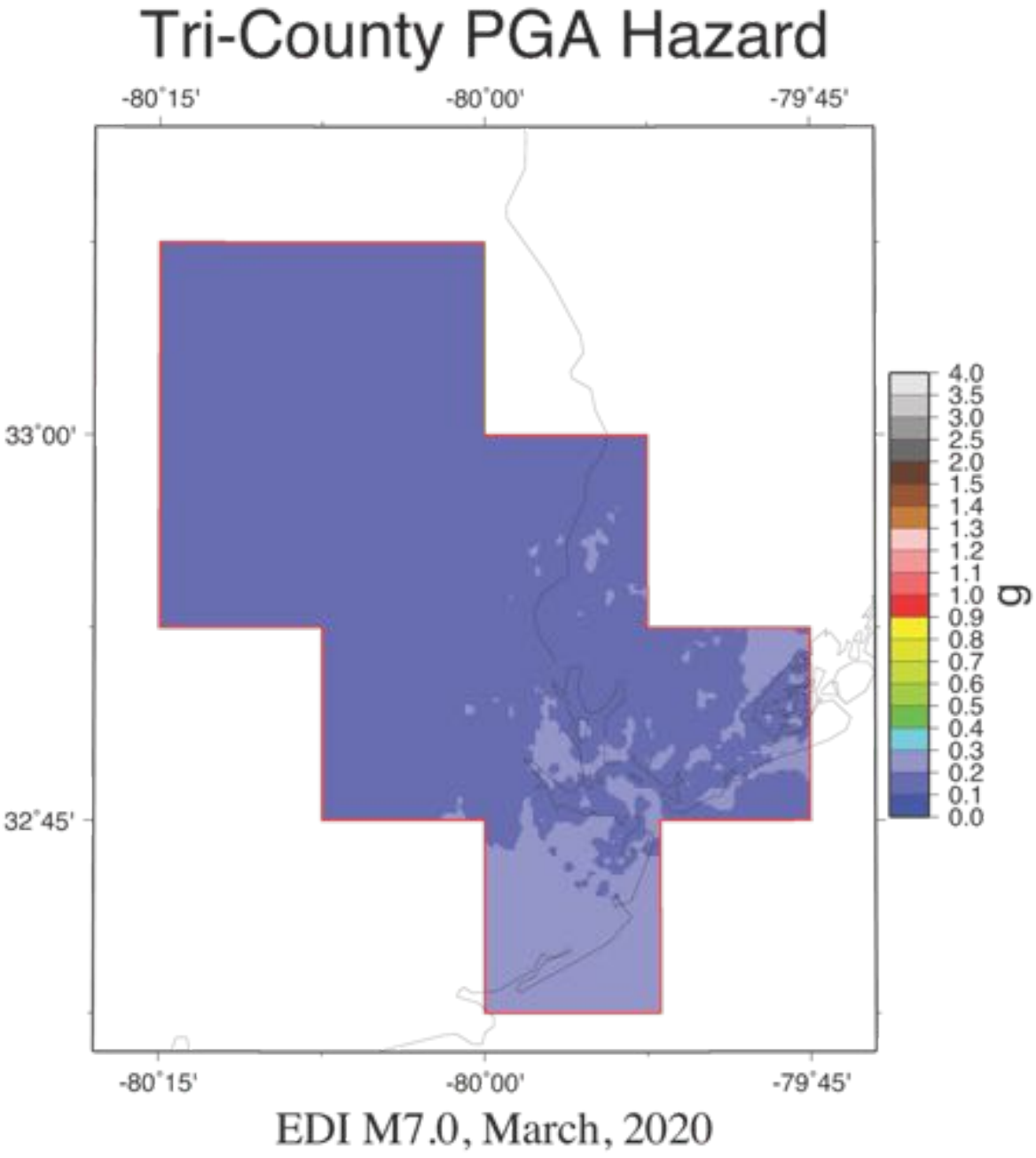

Figure 15a: PGA scenario seismic hazard map for all nine-quadrangles for a M7.0 in the offshore Edisto seismic area.

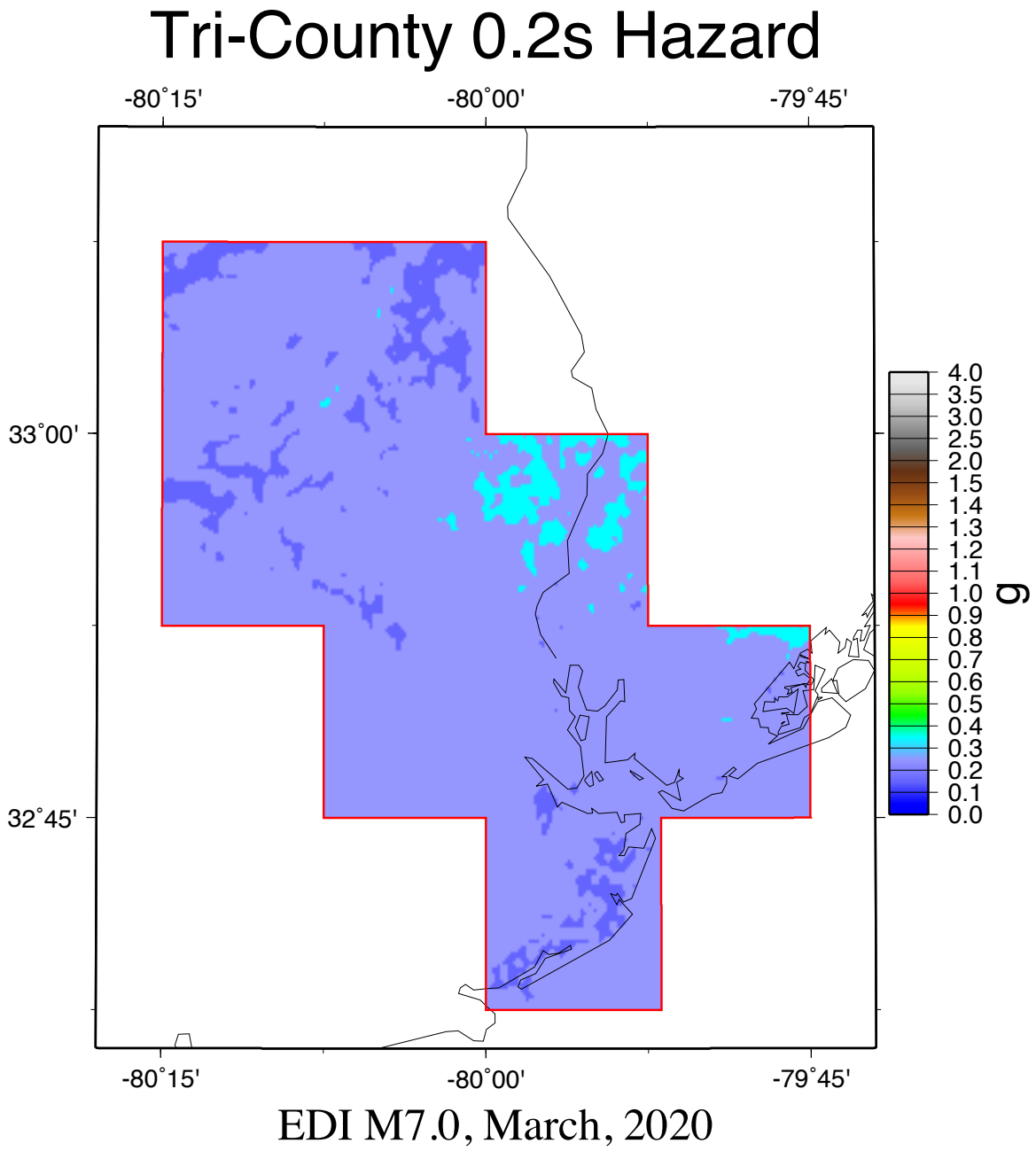

Figure 15b: 0.2 s scenario seismic hazard map for all nine-quadrangles for a M7.0 in the offshore Edisto seismic area.

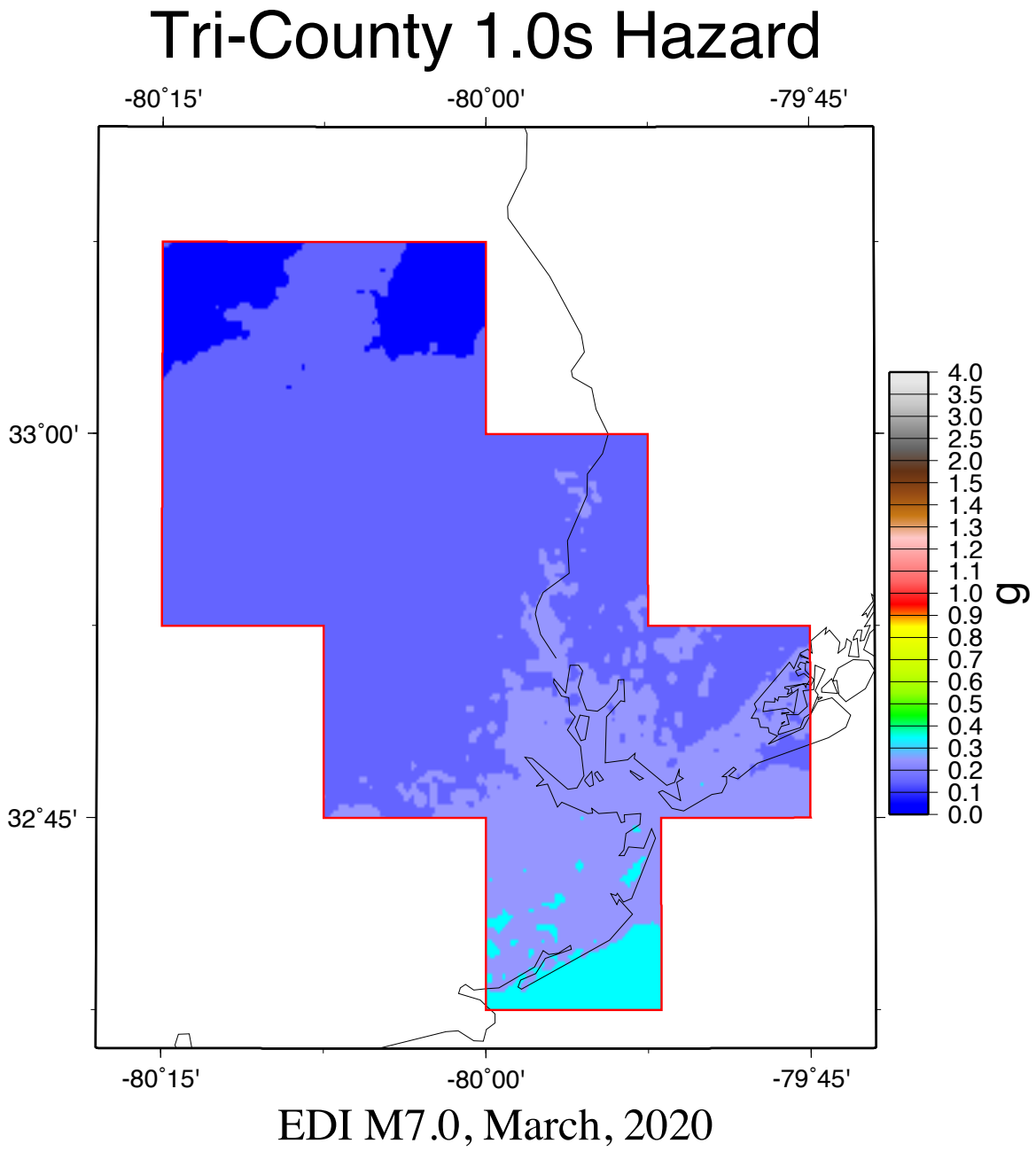

Figure 15c: 1.0 s scenario seismic hazard map for all nine-quadrangles for a M7.0 in the offshore Edisto seismic area.

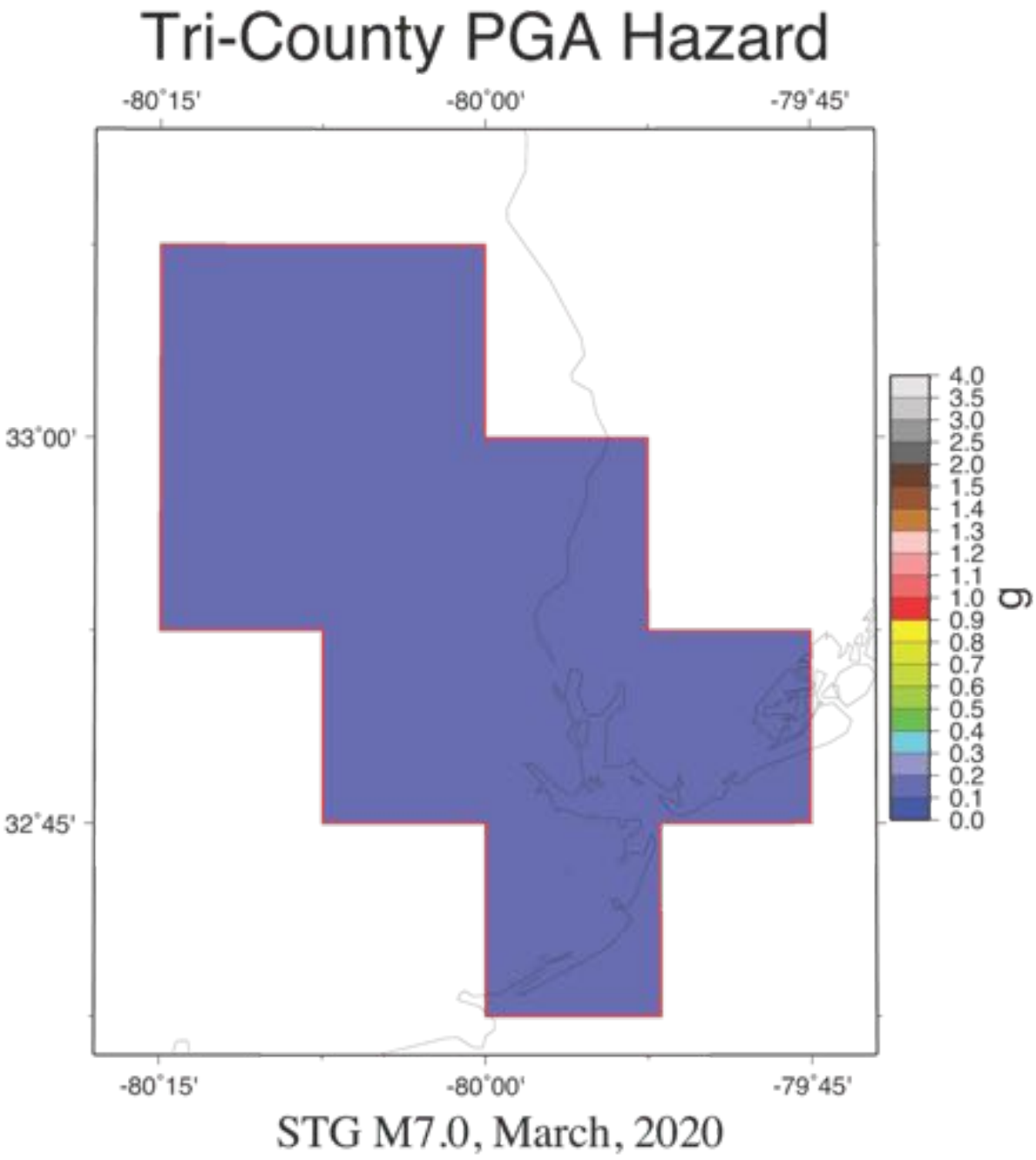

Figure 16a: PGA scenario seismic hazard map for all nine-quadrangles for a M7.0 in the St. George seismic area.

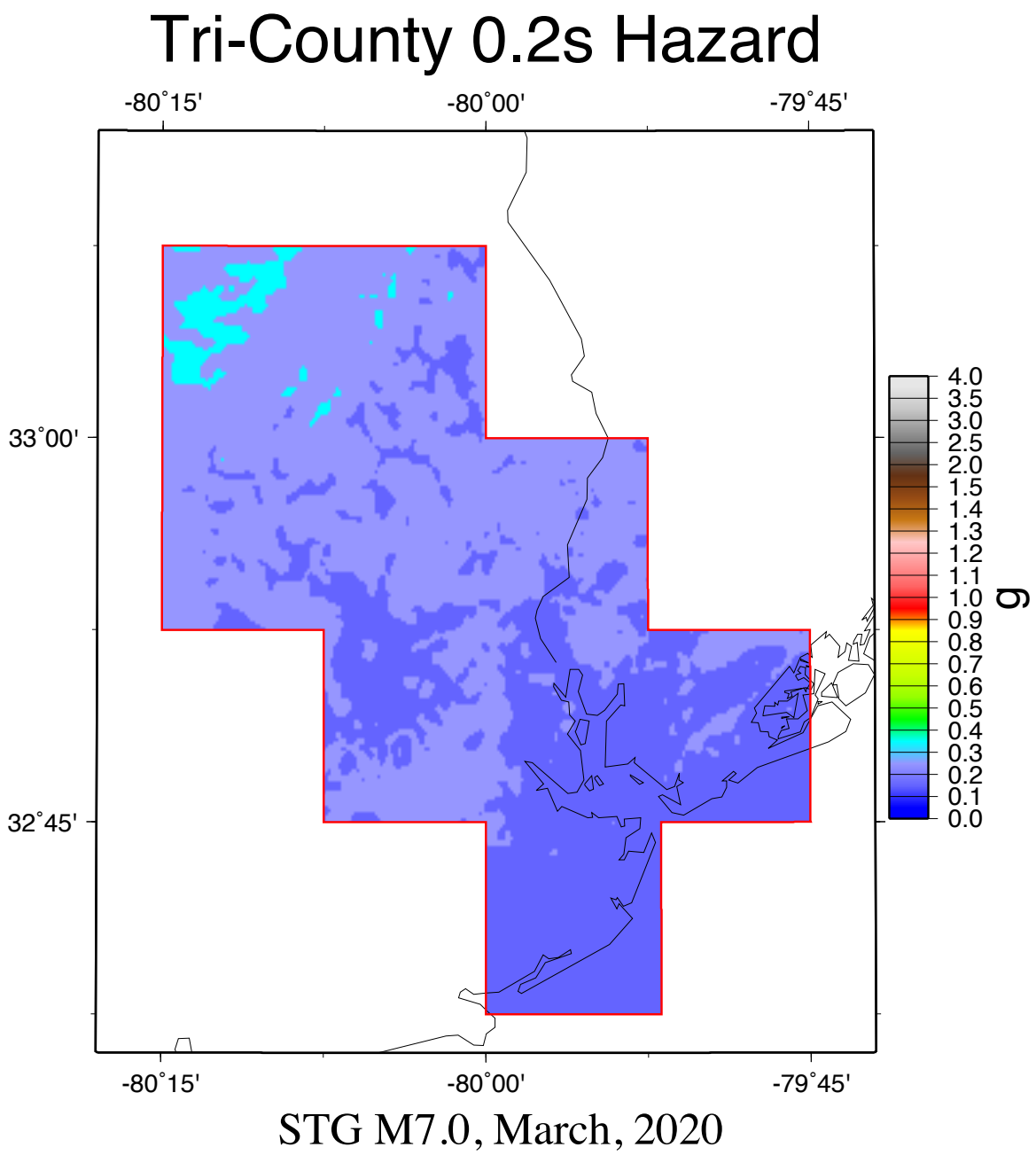

Figure 16b: 0.2 s scenario seismic hazard map for all nine-quadrangles for a M7.0 in the St. George seismic area.

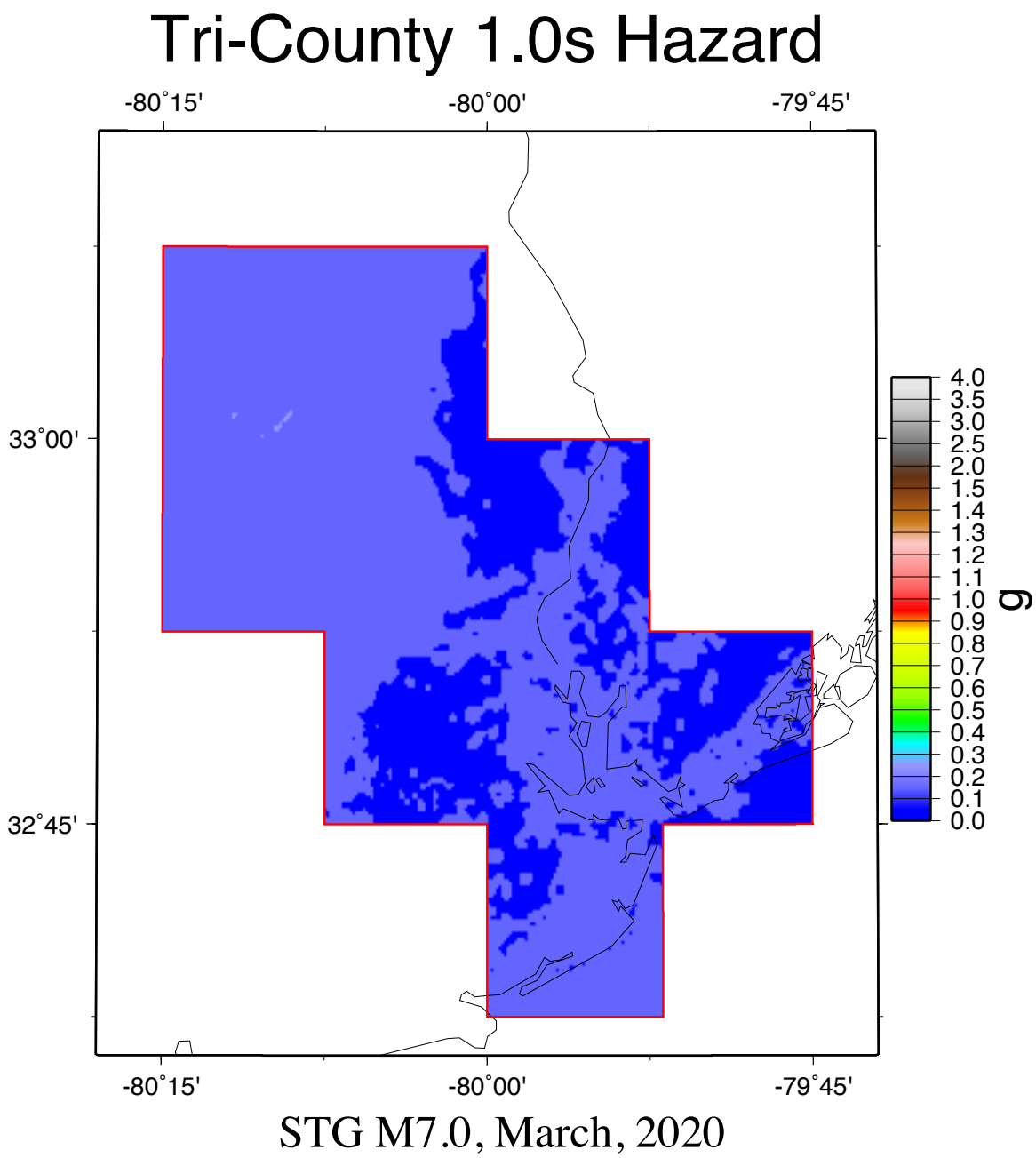

Figure 16c: 1.0 s scenario seismic hazard map for all nine-quadrangles for a M7.0 in the St. George seismic area.

Liquefaction Hazard Maps

We have produced liquefaction hazard maps for the likelihood of moderate or severe liquefaction. Both probabilistic and scenario liquefaction hazard maps have been generated using the approach described in the Methodology section for all the seismic hazard map types above.

Figure 17 presents the probabilistic liquefaction hazard maps for 2%-in-50y probability of exceedance. Figure 17 shows both the full nine-quadrangle hazard map and the zoomed-in portion of the map focusing on the Charleston Peninsula. The liquefaction hazard is very high next to rivers and near the Charleston Peninsula.

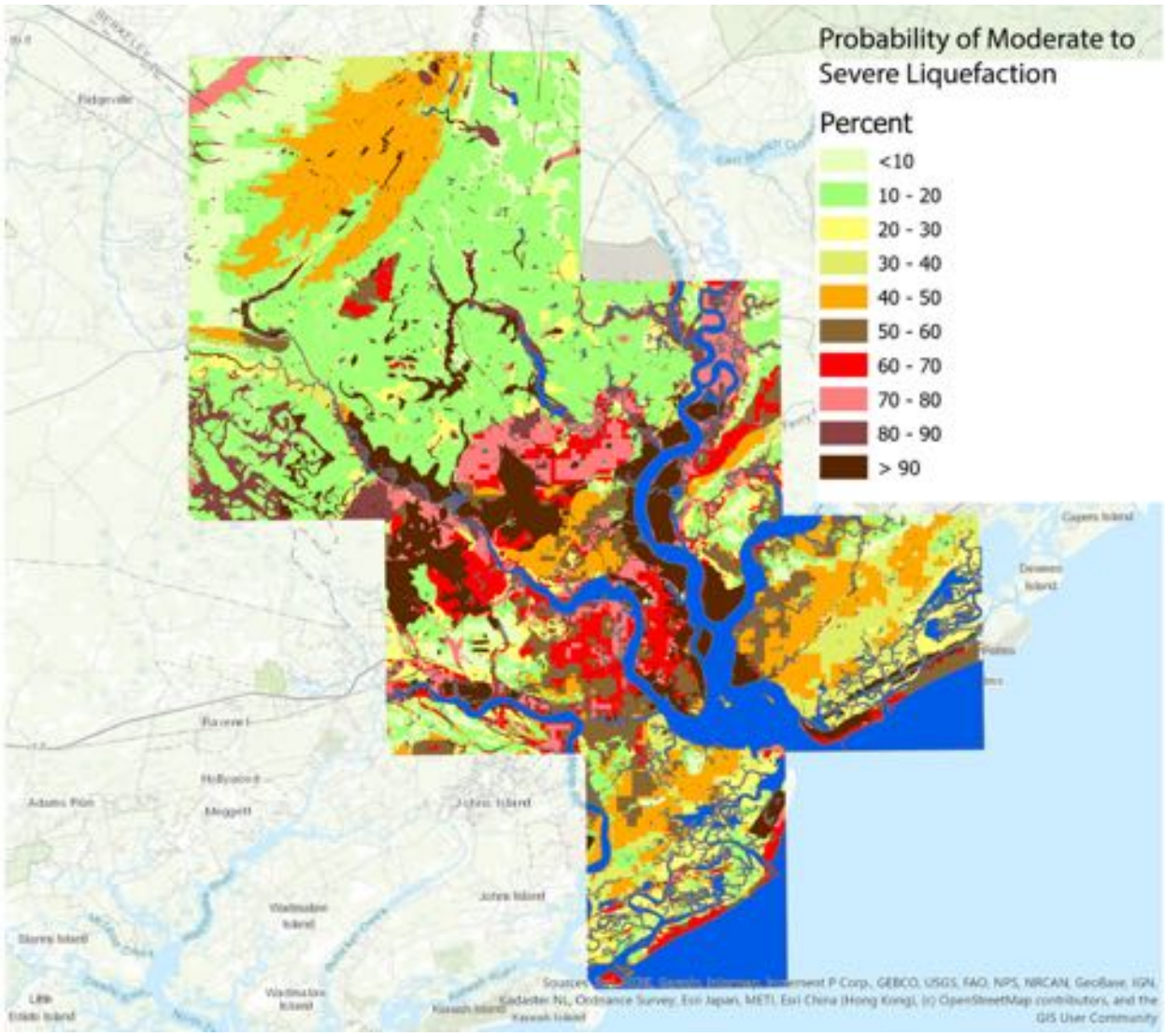

Figure 17a: 2%-in-50y probabilistic liquefaction hazard map for the nine-quadrangle study area.

2%-in-50y

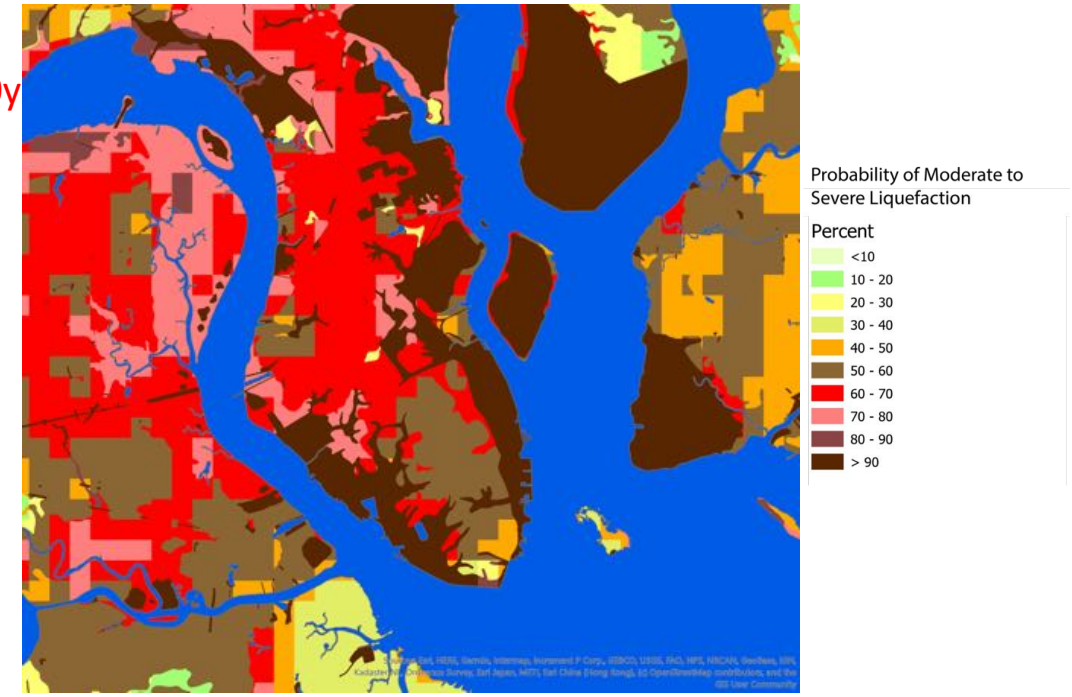

Figure 17b: 2%-in-50y probabilistic liquefaction hazard map for the Charleston Peninsula.

Figure 18 shows the M7.0 scenario liquefaction hazard maps for the Charleston seismic zone near Summerville. The hazard is low away from rivers and marshes, but high next to rivers and in marshy areas. Artificial fill in the Charleston area tends to be next to rivers and to fill in marshy area, which leads to high liquefaction hazard. The M7.0 scenario liquefaction hazard map best models the liquefaction observations from the 1886 M7.0 Charleston earthquake (Hayati and Andrus, 2008; Heidari and Andrus, 2010; Cramer et al., 2015).

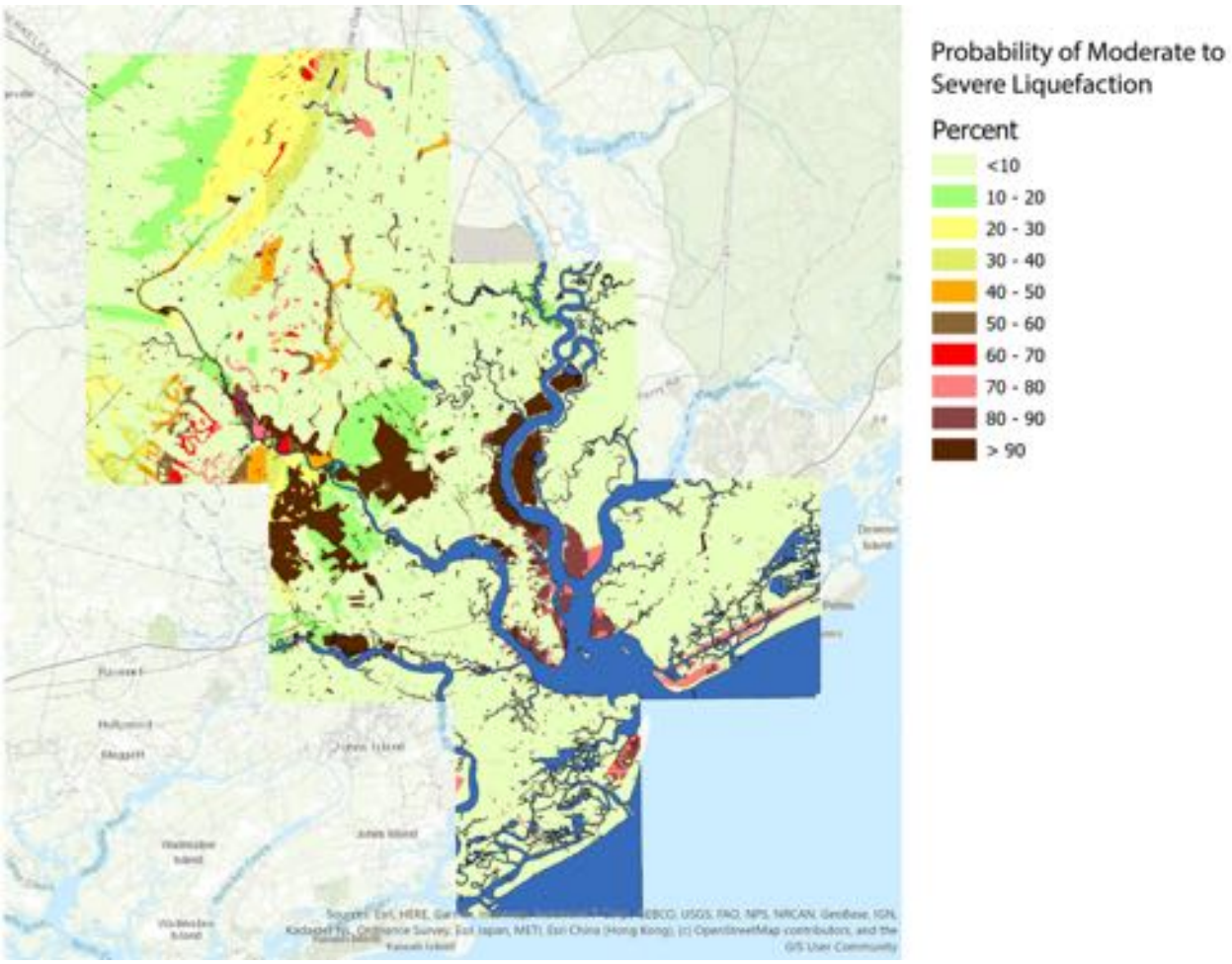

Figure 18a: Scenario liquefaction hazard map for the nine-quadrangle study area for a M7.0 in the Charleston seismic zone near Summerville.

M7.0

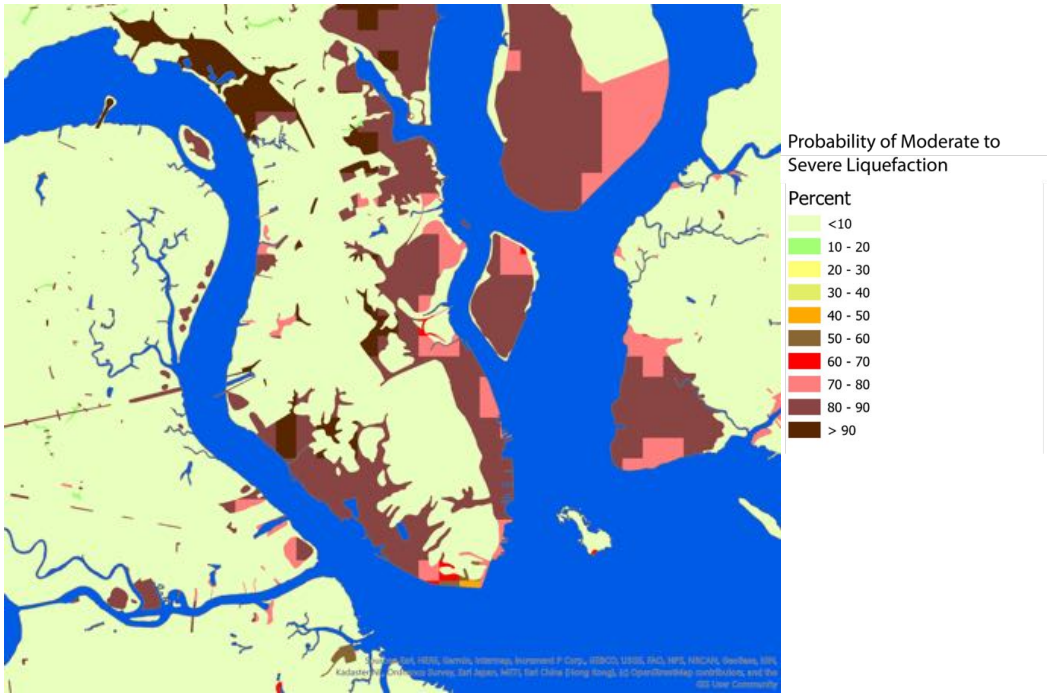

Figure 18b: Scenario liquefaction hazard map for the Charleston Peninsula for a M7.0 in the Charleston seismic zone near Summerville.

1886 Alternative Source Comparison

It turns out that there is not a good catalog of local intensity observations in the Charleston area from the 1886 M7.0 earthquake. Bakun et al (2002) and Bollinger (1977) report more on the far field intensity reports and their extent in distance from the source. There are few local reports of intensity listed in these two publications. This makes it difficult to compare the observations (converted to ground motion using a CEUS GMICE like Cramer, 2020) with the alternative 1886 source scenario maps we generated. However, as shown in Figure 19, Bollinger (1977) shows the sites and region of MMI X observations from the 1886 earthquake. The MMI X area is roughly triangular shaped with Summerville in the northwest corner, Ravenel in the southern corner, and the Cooper River east of Summerville as the east corner. This triangle will be used to represent the MMI X area in subsequent comparison figures with alternative M7.0 source scenarios. Note that the buildings and chimneys with MMI X damage (red circles in Figure 19) lie mainly in the western portion of the zone between Summerville and Ravenel, but are still too sparse for direct comparison to ground motion models.

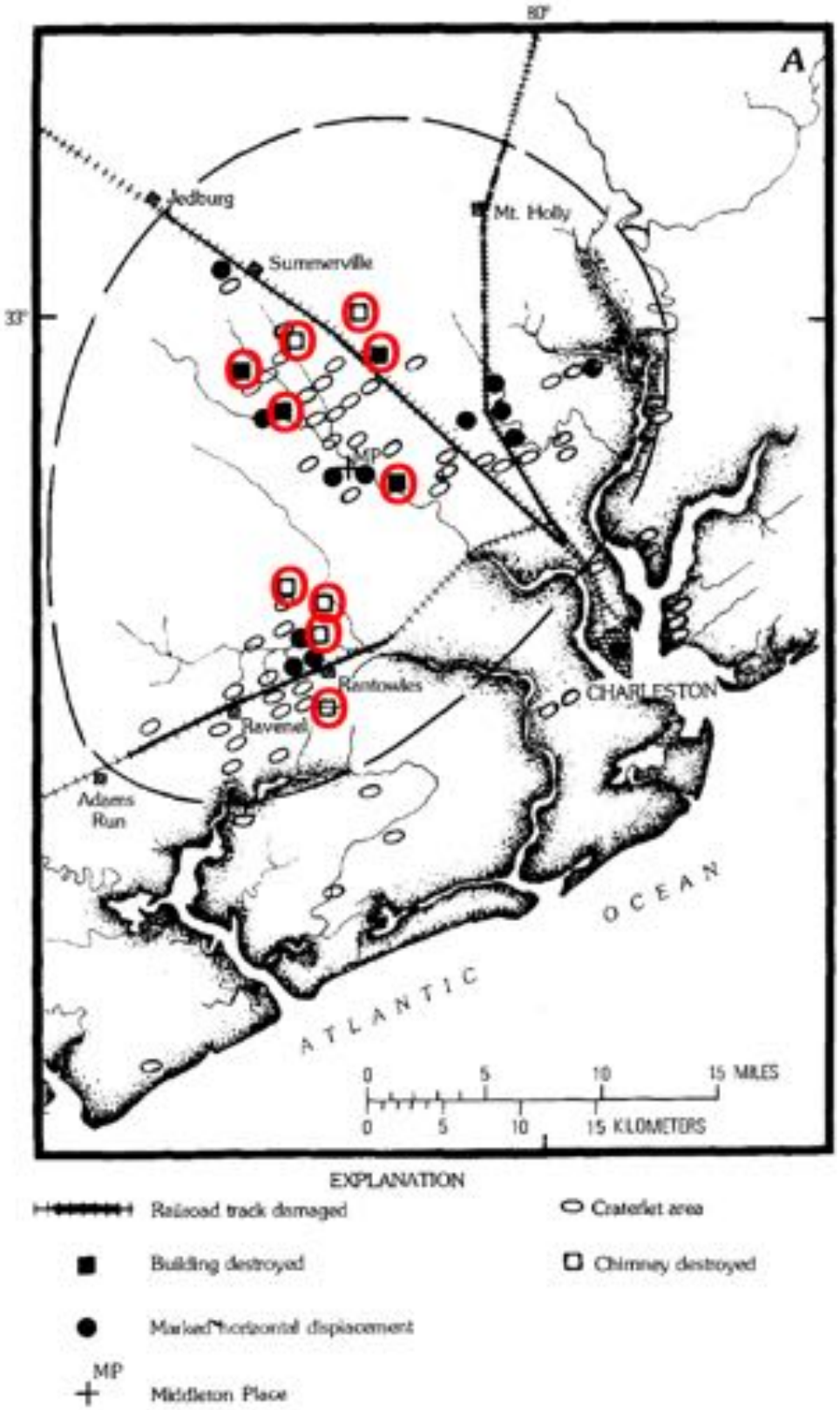

Figure 19: Area of MMI X for the 1886 Charleston earthquake from Bollinger (1977). Red circles highlight sites of building and chimney MMI X damage.

We use our triangular model of the MMI X region from Bollinger (1977) for comparison to our 1886 M7.0 alternative source scenario PGA hazard maps. The alternative source models are 1) a near Summerville vertical strike-slip fault striking NNE, 2) a west-dipping fault to the west of Summerville from Chapman et al. (2016) with similar strike, and 3) an offset at the Ashley River of the Woodstock vertical fault of Dura-Gomez and Talwani (2009) with similar strike. Figure 19 shows the M7.0 scenario PGA hazard maps from these three proposed alternative sources for the 1886 earthquake. From Figure 20 we see that all three alternative models are fairly compatible with the Bollinger MMI X region, particularly the western portion where the MMI X damaged buildings and chimneys are located. However, the west-dipping fault of Chapman et al. (2016) has its highest PGA region further west than the other two alternatives and thus appears to be a less likely source for the 1886 earthquake.

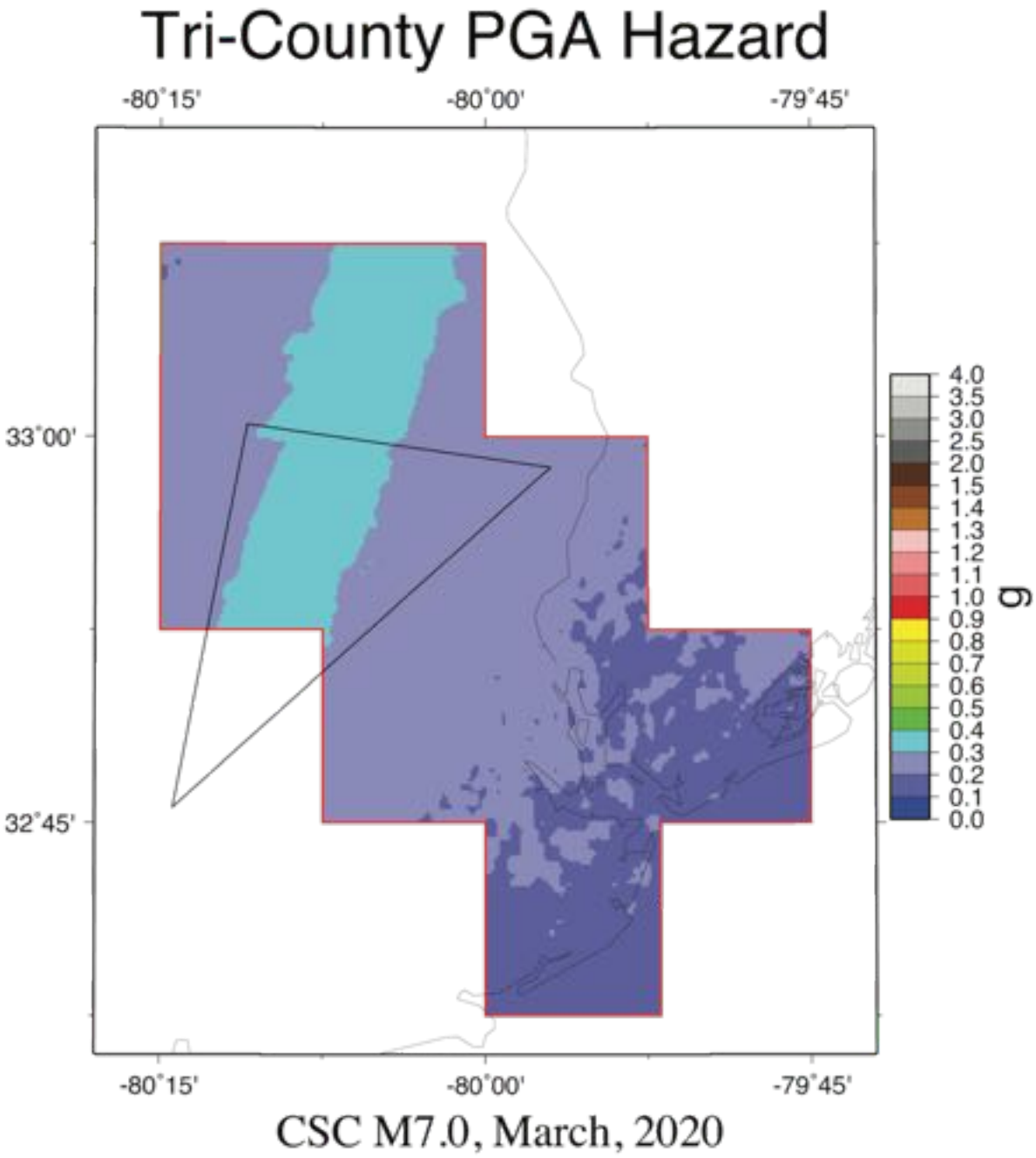

Figure 20a: Comparison of the Bollinger (1977) 1886 MMI X region (triangle) with the scenario PGA hazard map for a M7.0 on a vertical strike-slip fault in the Charleston seismic zone near Summerville.

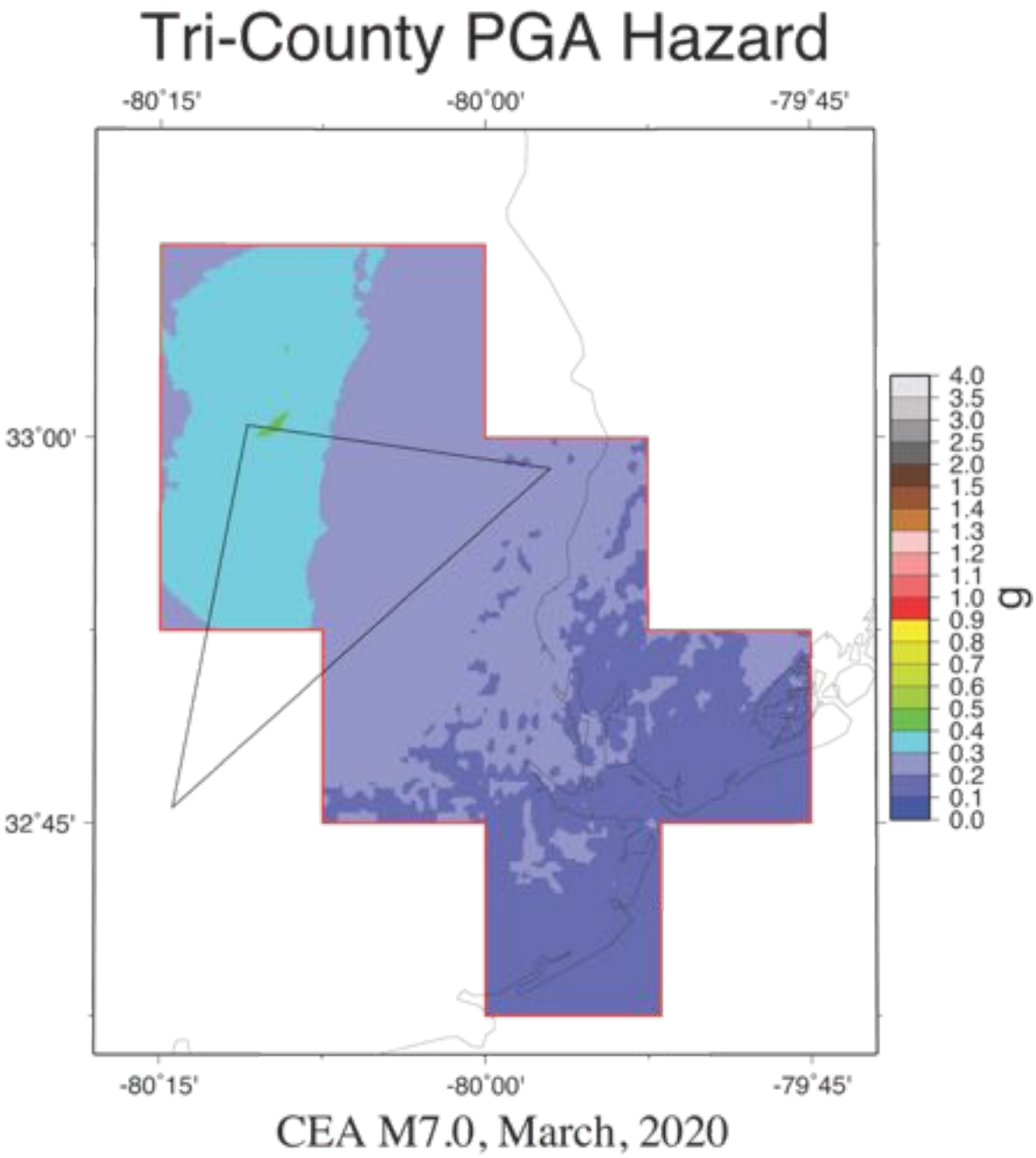

Figure 20b: Comparison of the Bollinger (1977) 1886 MMI X region (triangle) with the scenario PGA hazard map for a M7.0 on the west-dipping fault of Chapman et al. (2016) in the Charleston seismic zone near Summerville.

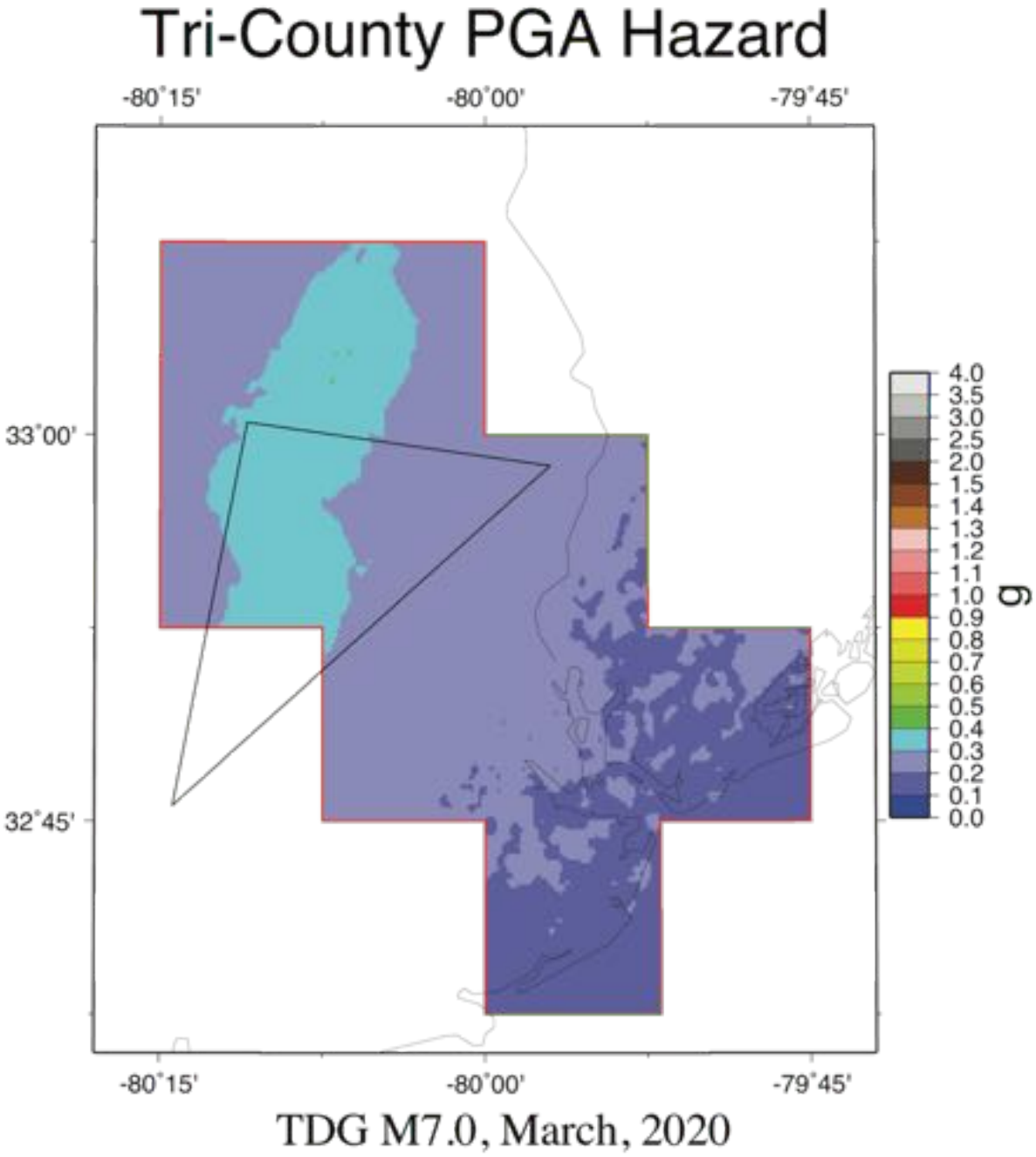

Figure 20c: Comparison of the Bollinger (1977) 1886 MMI X region (triangle) with the scenario PGA hazard map for a M7.0 on the offset Woodstock fault of Dura Gomez and Talwani (2009) in the Charleston seismic zone near Summerville.

Time History Database

The engineering community requested a time history database to assist with engineering analysis in the Charleston area (Cramer et al., 2015). The database of time histories is to be for the

Cooper Marl (Tertiary clay) at the surface. Cooper Marl is considered engineering "bedrock" in the Charleston Area. The time histories in the database is requested to be M7 only.

We conducted a sensitivity test to see the effects of the variations in the depth to bedrock and the higher velocity Gordon Formation in the CAEHMP study area. The depth to bedrock varies from 700 to 900 m across the study region. The depth to the top of the Gordon Formation (which has a fairly constant thickness of about 30m) varies from 50 to 120 m. We also looked at the sensitivity of response spectra to two alternative Vs models for the deeper sediments below the Pee Dee Formation. The Charleston Community Velocity Model specifies an average Vs for the sediments below the Pee Dee Formation. In the Charleston quadrangle pilot study (Cramer et al., 2015), we used the Chapman et al. (2006) Vs model for these deeper sediments.

Figure 21 shows the three Vs profiles used in the sensitivity test: Charleston, Summerville, and Mount Holly. Figure 22 presents the results of the sensitivity test. There is no significant difference in the response spectra for a given Vs profile between the two alternative deeper sediment velocity model (solid vs. dashed lines). For the depth to bedrock variations (longer periods above 1.0 s) there are only minor variations in the response spectra. For the variations in the depth to the top of the Gordon Formation, there is some variations at short period (between 0.1 and 1.0 s).

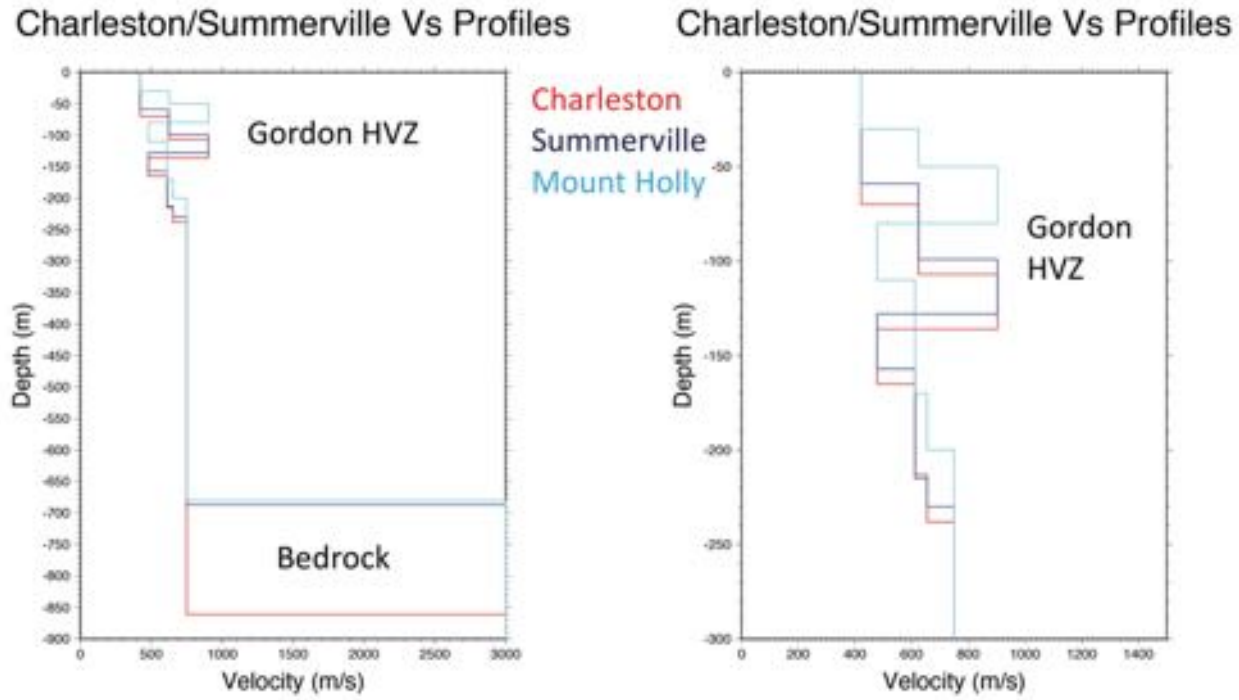

Figure 21: Three Vs profiles used in sensitivity test.

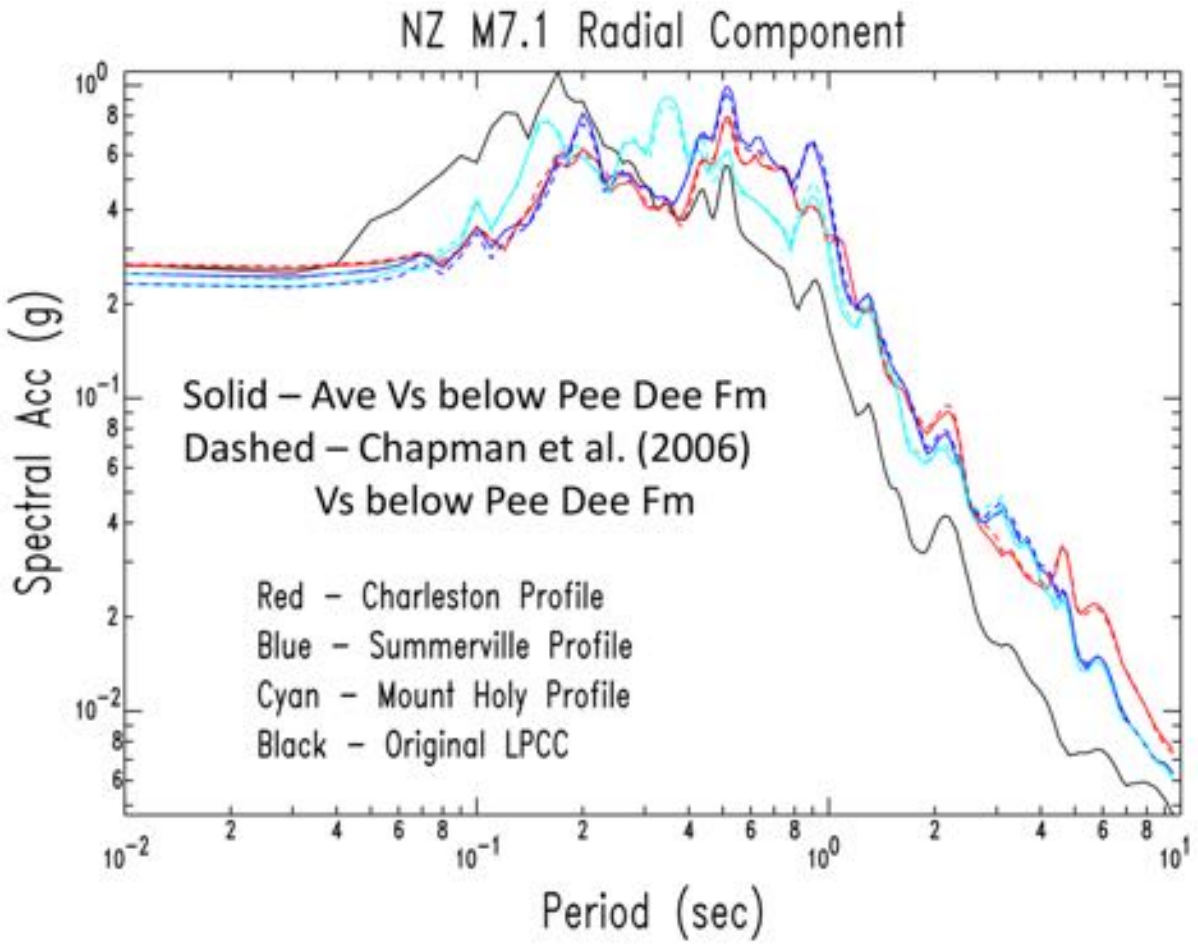

Figure 22: Original and modified response spectra from the sensitivity test.

A review was conducted by some members of the engineering community of the time histories developed during the sensitivity test. They used all the generated time histories in their engineering analysis procedures and concluded that there was no significant difference in the engineering results. This meant that there was no need for subdividing the time history database into different regions within the greater Charleston area. The conclusion by the engineering community test group was that a time history database based on just the Charleston Vs profile in Figure 21 is sufficient for their engineering needs.

Table 1 lists the ~M7 time histories from worldwide sources that were modified and included in the requested time history database. The resulting time histories are available from the LowCountry Hazard Center website (https://arcg.is/1nPWuy).

Table 1: Base time histories selected for the Charleston area time history database.

Selected Time Histories

Earthquake	Mag	Dist.	Fault Type	Soil Condition
• Darfield NZ	7.1	45 km	SS	B
• Gazli USSR	6.8	13 km	Thrust	Soil
• Nahanni	6.76	6-22 km	Thrust	Rock
• Cape Mendocino	7.1	10 km	Thrust	Rock
• Chi Chi Taiwan	7.6	17 km	Thrust	
• Duzce Turkey	7.1	26 km	SS	B
• Hector Mine	7.1	12 km	SS	B
• Kobe Japan	6.9	1 km	SS	B
• Kocaeli Turkey	7.4	7-11 km	SS	
• Loma Prieta	6.9	10 km	SS	
• Landers	7.3	2-11 km	SS	

Workshops

We initially planned for four stakeholder workshops, but wound up holding only three workshops. This was in part due to the federal government shutdown at the end of 2018/beginning of 2019, which prevented federal government stakeholders (including USGS staff) from participating initially. All workshops were held at the College of Charleston campus and stakeholders participated both in-person and online. The three workshops were:

April 3, 2019 Workshop: For this workshop only geoscience, engineering and geotechnical engineering professionals were invited. The main purpose of the workshop was to discuss which seismic and liquefaction hazard products that would be of most interest and use to the engineering and geotechnical engineering community in the greater Charleston region. The main result of this workshop was that an earthquake time history database of ground motion at the top of the Cooper Marl (i.e., a stiff clay that is used as engineering "bedrock" in the Charleston area) would be of the greatest value to this community (see Table 1 above).

August 1, 2019 Workshop: For this workshop a broader audience of stakeholders, primarily those involved in emergency management and regional planning were invited, in addition to the geoscience and engineering professionals invited to the first workshop. Some preliminary mapping products were presented; in addition we presented our research on the nature of the subsurface beneath the artificial fill on the Charleston Peninsula. An important outcome of this meeting was the decision to create an updated surface geology product for the Charleston quadrangle and to use it to make finer (~100 m) resolution maps for this quadrangle. Another important outcome was the decision to provide a range of earthquake scenario maps with different source regions and magnitudes.

December 6, 2019 Workshop: As in the August 1 workshop, a broad array of geoscience, engineering, emergency management and regional planning professionals were invited. At this workshop we presented near final seismic and liquefaction hazard maps and discussed the implications of results. Of particular interest to the regional planning and emergency management community was the differential impact of the multiple earthquake source/magnitude scenarios.

Conclusions

As part of the Charleston Area Earthquake Hazards Mapping Project, we developed under this grant seismic and liquefaction hazard maps, compared M7.0 scenario hazards from three alternative 1886 source faults with the MMI X area from Bollinger (1977), generated a time history database for Cooper Marl at the surface for use by the engineering community, and conducted four quarterly meetings with the Charleston area user community seeking their input and presenting our results. All products, including the previously developed community velocity and liquefaction probability models, are available from the Lowcountry Hazards Center website (https://arcg.is/1nPWuy).

While the thick soft sediments in the Charleston area can mitigate some of the seismic hazard due to nonlinear soil effects, the seismic hazard in the Charleston area is still high. Also, the liquefaction hazard depends on the surface geology type at a given site. Many areas away from rivers and marshes (filled and unfilled) show a low probability of moderate or severe liquefaction from M7.0 earthquakes in the Charleston seismic zone, those sites near rivers and on marshes (filled and unfilled) show high liquefaction hazard. Generally, the hazard maps were generated on a ~500m grid for the entire nine-quadrangle study area. Because of the greater amount and denser data available for the Charleston quadrangle, we developed hazard maps on a ~100 m grid for that quadrangle. Additionally, a comparison of M7.0 alternative source model PGA hazard maps with the MMI X area from the 1886 M7.0 Charleston earthquake indicated that all three alternative sources for the 1886 are fairly compatible with the observations, but the west-dipping fault shows a greater shift to the west in the highest PGA region relative to the MMI X observations that makes it a less likely alternative. Finally, we developed a M7 Charleston area time history database for the Cooper Marl at the surface at the request and for the use of the engineering community. Quarterly workshops for the user community explaining results and seeking feedback were conducted throughout 2019.

References

Andrus, R.D., Fairbanks, C.D., Zhang, J., Camp, W.M., Casey, T.J., Cleary, T.J., and Wright, W.B. (2006). "Shear-Wave Velocity and Seismic Response of Near-Surface Sediments in Charleston, South Carolina," *Bulletin of the Seismological Society of America*, **96**(5), 1897-1914.

Bakun, W.H., A.C. Johnston, and M.G. Hopper, 2002, Modified Mercalli intensities (MMI) for large earthquakes near New Madrid, Missouri, in 1811-1812 and near Charleston, South Carolina, in 1886, *U.S. Geol. Surv. Open-File Rept. 02-184*, 31 pp.

Bollinger, G.A., 1977, Reinterpretation of the intensity data for the 1886 Charleston, South Carolina, earthquake, in Rankin, D.W., ed., Studies related to the Charleston, South Carolina, earthquake of 1886 – A preliminary report, U.S. Geological Survey Professional Paper 1028, 17-32.

Bonilla, L. F., 2000, "Computation of linear and nonlinear site response for near field ground motion", Ph.D. Dissertation, University of California, Santa Barbara, 285 pp.

Bonilla, L. F., Archuleta R. J., Lavallee D., 2005, Hysteretic and Dilatant behavior of cohesionless soils and their effects on nonlinear site response: field data observations and modeling, *Bull. Seism. Soc. Am.* **95**, 2373–2395.

Chapman, M.C., and P. Talwani (2002). *Seismic hazard mapping for bridge and highway design in South Carolina*, Report to South Carolina Dept. of Transportation, December 26, 2002.

Chapman, M.C., J.R. Martin, C.G. Olgun, and J.N. Beale (2006). Site-response models for Charleston, South Carolina, and vicinity developed from shallow geotechnical investigations, *Bull. Seism. Soc. Am.* **96**, 467-489.

Chapman, M.C., J.N. Beale, A.C. Hardy, and Q. Wu, 2016, Modern seismicity and the fault responsible for the 1886 Charleston, South Carolina, earthquake, *Bull. Seism. Soc. Am.* **106**, 364-372.

Cramer, C.H., 2003, Site-specific seismic-hazard analysis that is completely probabilistic, *Bull. Seism. Soc. Am.* **93**, 1841-1846.

Cramer, C.H., 2005, Erratum: Site-specific seismic-hazard analysis that is completely probabilistic, *Bull. Seism. Soc. Am.* **95**, 2026.

Cramer, C.H., 2011, Final Technical Report, a proposal in support of the St. Louis Area Earthquake Hazards Mapping Project: Update to Methodology and Urban Hazard Map Uncertainty Analysis, USGS grant G09AP00008, February 14, 2011, CERI, 26 pp (available at http://earthquake.usgs.gov/research/external/reports/G09AP00008.pdf).

Cramer, C.H., 2014, Magnitude dependent site amplification seismic hazard calculation outside the hazard integral for St. Louis, MO (abstract), *Seism. Res. Lett.* **85**, 542.

Cramer, C.H., 2020, Updated GMICE for central and eastern North America extending to higher intensities, *Seism. Res. Lett.*, submitted.

Cramer, C.H., and O.S. Boyd, 2014, Why the New Madrid earthquakes are M 7-8 and the Charleston earthquake is ~M7, *Bull. Seism. Soc. Am.* **104**, 2884-2903.

Cramer, C.H., J.S. Gomberg, E.S. Schweig, B. A. Waldron, and K. Tucker, 2004, *Memphis, Shelby County, Tennessee, seismic hazard maps*, U.S. Geological Survey, Open-File Report 04-1294, 41pp.

Cramer, C.H., J.S. Gomberg, E.S. Schweig, B.A. Waldron, and K. Tucker, 2006, First USGS urban seismic hazard maps predict the effects of soils, *Seism. Res. Lett.* **77**, 23-29.

Cramer, C.H., G. Rix, and K. Tucker, 2008, Probabilistic liquefaction hazard maps for Memphis, Tennessee, *Seis. Res. Lett.* **79**, 392-399.

Cramer, C.H., S.C. Jaume, and N.S. Levine, 2015, Final Technical Report, Charleston Area Earthquake Hazards Mapping Project (CAEHMP) Workshop and Pilot Study: Collaborative Research with the College of Charleston and the University of Memphis, USGS grants G14AP00023 and G14AP00024, April 15, 2015, CERI, 46 pp (available at http://earthquake.usgs.gov/research/external/reports/G14AP00024.pdf).

Cramer, C.H., M.S. Dhar, and D. Arellano, 2018, Update of the urban seismic and liquefaction hazard maps for Memphis and Shelby County, Tennessee: liquefaction probability courves and 2015 hazard maps, *Seis. Res. Lett.* **89**, published online 3 January 2018.

Dhar, M.S., 2017, Probabilistic seismic hazard analysis of the Mississippi embayment incorporating nonlinear site effects, Ph.D. thesis, University of Memphis.

Dhar, M.S., and C.H. Cramer, 2017, Probabilistic seismic and liquefaction hazard analysis of the Mississippi embayment incorporating nonlinear effects, *Seis. Res. Lett.* **89**, 253-267, published online 13 December 2017.

Dura-Gomez, I., P. Talwani, 2009, Finding faults in the Charleston Area, South Carolina: 1. Seismological Data, *Seism. Res. Lett.* **80**, 883-900.

Dutch Dialogues Charleston, September 2019, 252 pp., https://www.dutchdialoguescharleston.org/.

EPRI, 1993, *Guidelines for determining design basis ground motions*, Electric Power Research Institute, Palo Alto, California TR-102293.

Hartzell, S., L.F. Bonilla, and R.A. Williams (2004). Predition of nonlinear soil effects, *Bull. Seism. Soc. Am.* **94**, 1609-1629.

Hayati, H., and Andrus, R.D. (2008). "Liquefaction Potential Map of Charleston, South Carolina Based on the 1886 Earthquake," *Journal of Geotechnical and Geoenvironmental Engineering*, **134**(6), 815-828.

Heidari, T., and Andrus, R.D. (2010). "Mapping Liquefaction Potential of Aged Soil Deposits in Mount Pleasant, South Carolina," *Engineering Geology*, **112**(1-4), 1-12.

Jaumé, S. C. (2006). Shear wave velocity profiles via SCPT and ReMi techniques at ANSS strong motion sites in Charleston, South Carolina

Jaumé, S. C. and K. S. Miner (2011). Seismic site amplification in Charleston, South Carolina: Modeling and Interpretation (abstract), *Seism. Res. Lett.* **82**, 315.

Jaumé, S. C., R. D. Andrus, M. Chapman, C. D. Fairbanks, N. P. Mohanan and L. A. Simonson (2015). Preliminary community velocity model for an urban hazard map pilot study in the greater Charleston, SC region, *Seism. Res. Lett.* **86A**, 517-518.

Jaumé, S. C., N. S. Levine, A. Braud and T. Howard (2016). Community velocity model for the Charleston Area Earthquake Hazard Mapping Project (CAEHMP): Data collection, integration and initial results, *Seism. Res. Lett.* **88**, 250.

Jaumé, S. C., and N. S. Levine (2018). Development of a community velocity model for the Charleston, South Carolina region, Final Technical Report, USGS NEHRP Award G16A00025, https://earthquake.usgs.gov/cfusion/external_grants/reports/G16AP00025.pdf.

Jaumé, S. C., R. Desilets and N. S. Levine (2019). Remapping Charleston: Using historical information to update seismic site conditions in an urban setting, *91st Meeting of the Eastern Section of the Seismological Society of America*, The Ohio State University, Columbus, Ohio, 3-5 November 2019, pp. 17-18.

Juang, C.H., and D.K. Li (2007). Assessment of liquefaction hazard in Charleston quadrangle, South Carolina, *Engineering Geology*, doi: 10.1016/j.enggeo.2007.03.003.

Lee, R.C., 2000, A methodology to integrate site response into probabilistic seismic hazard analysis, Site Geotechnical Services, Savannah River Site, report of 3 February 2000.

Miner, K. S. and S. C. Jaumé (2011). Seismic site amplification in Charleston, South Carolina: Observations (abstract), *Seism. Res. Lett.* **82**, 315.

Motazedian, D., K. Khaheshi Banab, J. A. Hunter, S. Sivathayalan, H. Crow and G. Brooks (2011). Comparison of site periods derived from different evaluation methods, *Bull. Seism. Soc. Am.* **101**, 2942-2954.

Ogweno, L.P., and C.H. Cramer, 2017, Improved CENA regression relationships between modified Mercalli intensities and ground-motion parameters, *Bull. Seism. Soc. Am.* **107**, 180-197.

Petersen, M. D., M. Moschetti, P. Powers, C. Mueller, K. Haller, A. Frankel, Y. Zeng, S. Rezaeian, S. Harmsen, O. Boyed, N. Field, R. Chen, K. Rukstales, N. Luco, R. Wheeler, R. Williams, and A. Olsen, 2014, *The 2014 update of the United States national seismic hazard models*, U.S. Geological Survey, OFR 2014-X1091, 255 p.

Petersen, M.D., A.M. Shumway, P.M. Powers, C.S. Mueller, M.P. Moschetti, A.D. Frankel, S. Rezaeian, D.E. McNamara, N. Luco, O.S. Boyd, K.S. Rukstales, K.S. Jaiswal, E.M. Thompson, S.M. Hoover, B.S. Clayton, E.H. Field, Y. Zeng, 2019, *Eqk. Spectra*, doi 10.1177/8755293019878199.

Pratt, T.L., A.K. Shah, J.W. Horton Jr., M.C. Chapman, and J. Beale, Recent fault activity in the 1886 Charleston, South Carolina earthquake epicentral area and it relation to buried structures (abstract), American Geophysical Union, Fall Meeting 2014, abstract id. T12B-07.

Reiter, L., 1990, *Earthquake Hazard Analysis: Issues and Insights*, Columbia University Press, New York.

Shi, J., and D. Asimaki, 2017, From stiffness to strength: formulation and validation of a hybrid hyperbolic nonlinear soil model for site-response analyses, *Bull. Seism. Soc. Am.* **107**, published online April 4, 2017, doi: 10.1785/0120150287.

Silva, W., I. Wong, T. Siegel, N. Gregor, R. Darragh, and R. Lee (2003). Ground motion and liquefaction simulation of the 1886 Charleston, South Carolina, earthquake, *Bull. Seism. Soc. Am.* **93**, 2717-2736.

Talwani, P., and W. T. Schaeffer (2001). Recurrence rates of large earthquakes in the South Carolina coastal plain based on paleoliquefaction data, *J. Geophys. Res.* **106**, 6621-6642.